JOURNAL OF GEOPHYSICAL RESEARCH, VOL. 104, NO. B3, PAGES 4835–4859, MARCH 10, 1999

Estimation of nutation using the Global Positioning System

M. Rothacher and G. Beutler

Astronomical Institute, University of Berne, Berne, Switzerland

Thomas A. Herring

Department of Earth, Atmospheric and Planetary Sciences, Massachusetts Institute of Technology, Cambridge

R. Weber

Department of Theoretical Geodesy, University of Technology Vienna, Vienna, Austria

Abstract. In the past the estimation of corrections to nutation models was uniquely reserved to very long baseline interferometry (VLBI) and lunar laser ranging (LLR) data processing. Although satellite space-geodetic measurements have been used to determine UT1-UTC rates (or length of day) for many years now, the estimation of nutation rates was not performed. There is no fundamental difference, however, between the estimation of rates in UT1-UTC and nutation rates in obliquity and longitude from satellite data. A simple variance-covariance analysis shows that significant contributions to nutation by the Global Positioning System (GPS) are possible for periods below about 16 days. Since March 1994, daily nutation rates have been computed at the Center for Orbit Determination Europe using the data collected by the global GPS network. The series of nutation rates now covers 3.5 years. It is used to compute corrections for a set of 34 nutation periods between 4 and 16 days. The formal uncertainties of the estimated nutation coefficients in obliquity $\Delta\epsilon$ and longitude $\Delta\psi \sin\epsilon_0$ grow linearly with period from several microarcseconds (μas) at periods of a few days to about 30 μas at periods of 16 days. The comparison of the GPS-derived coefficients with the International Earth Rotation Service 1996 nutation model shows an overall agreement of 10 μas (median). The GPS results are also in very good agreement with the most recent model by Souchay and Kinoshita (1997.2), better than most of the VLBI and LLR results reported in the literature. GPS thus allows, although limited to high frequencies because of the satellite orbits involved, an independent check of the validity of theoretical nutation models and of results obtained from VLBI and LLR.

1. Introduction

The Center for Orbit Determination in Europe (CODE) is one of seven analysis centers of the International Global Positioning System (GPS) Service for Geodynamics (IGS) [see, e.g., *Beutler et al.*, 1994a; *Zumberge et al.*, 1997]. CODE, a cooperation of the Astronomical Institute, University of Berne (Switzerland), the Swiss Federal Office of Topography, Wabern (Switzerland), the Bundesamt für Kartographie und Geodäsie, Frankfurt (Germany), and the Institut Géographique National, Paris (France), has participated in the activities of the IGS since June 1992, analyzing on a daily basis the data of the global IGS network (approximately 90 GPS receivers are analyzed by CODE in 1997) to obtain high-precision satellite ephemerides and satellite clocks, series of Earth orientation parameters (EOP), coordinates and velocities of the sites, and information concerning the atmosphere (troposphere and ionosphere).

CODE was the first IGS analysis center to routinely estimate UT1-UTC rates from the global GPS data in June 1992. Soon the other analysis centers followed this example. In February 1994, CODE started to derive celestial pole offset parameters (nutation rates). These estimates were thought to prove or disprove the idea that GPS as a satellite technique is able to contribute to nutation. Results of a first analysis of nutation rates from CODE, including the estimation of corrections to some of the short-period nutation terms (below 30 days) relative to the International Astronomical Union (IAU) 1980 Theory of Nutation, were presented at the International Earth Rotation Service (IERS) workshop in Paris in 1995 and documented by *Weber* [1996].

In this article we give an overview of the contributions to nutation we may obtain from satellite techniques and GPS in particular. In the next section we discuss the application of nutation rates compared with nutation offsets. The subsequent sections give a brief overview of GPS data processing necessary to obtain nutation rate estimates (section 3), dis-

Paper number 1998JB900078.
0148-0227/99/1998JB900078$09.00

cuss the problem of correlations of orbit model parameters with nutation rates (section 4.2), and describe the analysis of the nutation rate values including the determination of nutation amplitudes for high-frequency nutation terms (section 5). Section 6, finally, contains the results obtained from GPS and the comparison with very long baseline interferometry (VLBI) and lunar laser ranging (LLR) nutation series.

2. Contribution of GPS to Nutation Series

The transformation between the Earth-fixed International Terrestrial Reference System (ITRS) and the International Celestial Reference System (ICRS) may be described by the following rotation matrix $\boldsymbol{R}$ [see, e.g., *McCarthy*, 1996]:

$$\boldsymbol{R} = \boldsymbol{P}(t)\,\boldsymbol{N}(t)\,\boldsymbol{R}_3(-\Theta)\,\boldsymbol{R}_1(y)\,\boldsymbol{R}_2(x) \qquad (1)$$

where t is observation epoch in terrestrial time (TT), $\boldsymbol{P}(t)$ and $\boldsymbol{N}(t)$ are the precession and nutation matrices at epoch t, $\boldsymbol{R}_i(\alpha)$ is a matrix describing a rotation around the axis i by the angle α, Θ is Greenwich True Sidereal Time at epoch t, and x, y are the coordinates of the Celestial Ephemeris Pole in the terrestrial reference system (ITRS) at epoch t.

The nutation matrix $\boldsymbol{N}(t)$ at epoch t is given by

$$\boldsymbol{N}(t) = \boldsymbol{R}_1(-\epsilon_0)\,\boldsymbol{R}_3(\Delta\psi)\,\boldsymbol{R}_1(\epsilon_0 + \Delta\epsilon) \qquad (2)$$

where ϵ_0 is the mean obliquity of the ecliptic at epoch t and $\Delta\epsilon$ and $\Delta\psi$ are the nutation angles in obliquity and longitude (referring to the mean pole at J2000, which is slightly offset from the ICRS pole [*Feissel and Castrique*, 1997]).

The Greenwich True Sidereal Time Θ is related to UT1-UTC through

$$\Theta = \Theta_m + \Delta\psi\,\cos\epsilon_0 + k_1\,\sin\Omega + k_2\,\sin 2\Omega \qquad (3)$$

$$\Theta_m = \Theta_m^0 + \rho\,\Delta\mathrm{UT1} \qquad (4)$$

$$\Delta\mathrm{UT1} = \Delta\,((\mathrm{UT1\text{–}UTC}) + \mathrm{UTC}) \qquad (5)$$

where Θ_m is Greenwich Mean Sidereal Time, Θ_m^0 is Greenwich Mean Sidereal Time at 0 hours UT1 of the day of observation, k_1 and k_2 are coefficients given, for example, by *Aoki and Kinoshita* [1983] or *McCarthy* [1996], Ω is the mean longitude of the ascending node of the lunar orbit, ρ is the ratio of universal time to sidereal time ($\rho \approx 1.0027379$), and ΔUT1 is the time interval from 0h UT1 to the observation epoch t in UT1.

The term "Earth Orientation Parameters" (EOP) comprises a set of five parameters, namely, the nutation offsets in $\Delta\epsilon$ and $\Delta\psi$, the pole coordinates x and y, and UT1-UTC, describing the rotation between the ITRS and ICRS given above. With the term "Earth Rotation Parameters" (ERP) we denote the subset $\{x, y, \mathrm{UT1\text{-}UTC}\}$.

The nutation theory officially adopted at present is still the IAU 1980 Theory of Nutation, which is based on Kinoshita's rigid Earth theory [*Kinoshita*, 1977] and Wahr's nonrigid theory [*Wahr*, 1981], that uses the Earth model 1066A. Wahr's theory deduces the ratio of the nutation amplitudes for the nonrigid Earth to those for the rigid model. Soon after the adoption of the IAU 1980 Theory of Nutation, VLBI (and LLR) observations revealed deficiencies in this theory at the level of several milliarcseconds (mas). Up to now VLBI and LLR were the only techniques capable of measuring nutation terms [e.g., *Charlot et al.*, 1995]. For the low-frequency part of the spectrum this will also be true in the future. (An exception may be the satellite laser ranging (SLR) considerations on the free core nutation mentioned by *Tapley et al.* [1993].)

Three of the EOP components, namely, UT1-UTC, $\Delta\epsilon$, and $\Delta\psi$, are not directly accessible to space geodetic techniques. All systems (VLBI, LLR, GPS, etc.) measure changes in these three components. In the case of VLBI these changes are determined relative to a very stable inertial coordinate frame. LLR realizes the inertial frame through the dynamics of the lunar orbit. The orbit of the moon can be modeled very well over long time spans and thus represents a reasonably stable reference frame. Due to the large nongravitational forces acting on artificial satellites, which are very difficult to model, an "inertial frame" may only be accurately established over a short time span (e.g., a few revolutions or a few days).

We first show that there is almost a one-to-one correspondence between changes in the orbital elements on one hand and the nutation angles $\Delta\epsilon$ and $\Delta\psi$ and a change in UT1-UTC on the other hand, or, stated differently, that it is not possible to estimate both, orbital elements for each satellite and offsets in nutation and UT1-UTC.

The position $\boldsymbol{r}_S$ of a satellite in the Earth-fixed system in the Keplerian approximation (no perturbation forces) may be computed as [see, e.g., *Beutler et al.*, 1996a]:

$$\boldsymbol{r}_S = \boldsymbol{R}_2(-x)\,\boldsymbol{R}_1(-y)\,\boldsymbol{R}_{\mathrm{eop}}(\Theta, \Delta\epsilon, \Delta\psi)\cdot \cdot\boldsymbol{R}_{\mathrm{orb}}(\Omega, i, u_0)\begin{pmatrix} r\cos(u-u_0) \\ r\sin(u-u_0) \\ 0 \end{pmatrix} \qquad (6)$$

with the notation

$$\boldsymbol{R}_{\mathrm{eop}}(\mathrm{UT1\text{–}UTC}, \Delta\epsilon, \Delta\psi) = \boldsymbol{R}_3(\Theta)\,\boldsymbol{R}_1(-\epsilon_0 - \Delta\epsilon)\,\boldsymbol{R}_3(-\Delta\psi)\,\boldsymbol{R}_1(\epsilon_0)\,\boldsymbol{P}^T \qquad (7)$$

$$\boldsymbol{R}_{\mathrm{orb}}(\Omega, i, u_0) = \boldsymbol{R}_3(-\Omega)\,\boldsymbol{R}_1(-i)\,\boldsymbol{R}_3(-u_0) \qquad (8)$$

where Ω is the right ascension of the ascending node of the satellite's orbit, i is the inclination of the orbit with respect to the equator, u is the argument of latitude of the satellite, u_0 is the argument of latitude at the osculation epoch of the orbital elements, and r is the distance of the satellite from the Earth's center.

Looking at (6) we immediately see that a net rotation due to offsets in $\Delta\epsilon$, $\Delta\psi$, and UT1-UTC may be absorbed by changing the rotation matrices $\boldsymbol{R}_3(-\Omega)$, $\boldsymbol{R}_1(-i)$, and $\boldsymbol{R}_3(-u_0)$, because any net rotation may be represented by three rotations around the three Eulerian angles Ω, i, and u_0. However, it is worthwhile to derive the formulas linking the changes (Δ(UT1–UTC), $\delta\Delta\epsilon$, $\delta\Delta\psi$) in the angles $\Delta\epsilon$, $\Delta\psi$, and UT1-UTC with the changes ($\Delta\Omega, \Delta i, \Delta u_0$) in the orbital elements Ω, i, and u_0.

Taking into account that $\Delta\epsilon$ and $\Delta\psi$ as well as $\delta\Delta\epsilon$, $\delta\Delta\psi$, and Δ(UT1–UTC) are small angles and assuming that the precession matrix $\boldsymbol{P}$ only contains small rotation angles (i.e., $\sin\alpha \approx \alpha$ and $\cos\alpha \approx 1$), we may write

$$\boldsymbol{R}_{\text{eop}}(\text{UT1–UTC} + \Delta(\text{UT1–UTC}), \Delta\epsilon + \delta\Delta\epsilon, \Delta\psi + \delta\Delta\psi) = \boldsymbol{R}_{\text{eop}}(\text{UT1–UTC}, \Delta\epsilon, \Delta\psi) \cdot \cdot \boldsymbol{D}_{\text{eop}}(\Delta(\text{UT1–UTC}), \delta\Delta\epsilon, \delta\Delta\psi) \quad (9)$$

with the rotation matrix $\boldsymbol{D}_{\text{eop}}$:

$$\boldsymbol{D}_{\text{eop}} = \begin{pmatrix} 1 & d_{12} & d_{13} \\ -d_{12} & 1 & d_{23} \\ -d_{13} & -d_{23} & 1 \end{pmatrix} \quad (10)$$

where

$$d_{12} = \Delta\Theta - \delta\Delta\psi \cos\epsilon_0 \quad (11a)$$
$$d_{13} = -\delta\Delta\psi \sin\epsilon_0 \quad (11b)$$
$$d_{23} = -\delta\Delta\epsilon \quad (11c)$$

Using (3) and (4) we may replace the change $\Delta\Theta$ in true sidereal time in (11a) by a change $\Delta(\text{UT1–UTC})$ in UT1-UTC:

$$d_{12} = \Delta\Theta - \delta\Delta\psi \cos\epsilon_0 = \Delta\Theta_m = \rho\,\Delta(\text{UT1–UTC}) \quad (12)$$

Small changes in the orbital orientation ($\Delta\Omega$, Δi, Δu_0), on the other hand, may be put into a similar matrix $\boldsymbol{D}_{\text{orb}}$,

$$\boldsymbol{R}_{\text{orb}}(\Omega + \Delta\Omega, i + \Delta i, u_0 + \Delta u_0) = \boldsymbol{D}_{\text{orb}}(\Delta\Omega, \Delta i, \Delta u_0)\, \boldsymbol{R}_{\text{orb}}(\Omega, i, u_0) \quad (13)$$

where

$$\boldsymbol{D}_{\text{orb}} = \begin{pmatrix} 1 & \delta_{12} & \delta_{13} \\ -\delta_{12} & 1 & \delta_{23} \\ -\delta_{13} & -\delta_{23} & 1 \end{pmatrix} \quad (14)$$

and

$$\delta_{12} = -\Delta\Omega - \cos i\, \Delta u_0 \quad (15a)$$
$$\delta_{13} = \sin\Omega\, \Delta i - \sin i \cos\Omega\, \Delta u_0 \quad (15b)$$
$$\delta_{23} = -\cos\Omega\, \Delta i - \sin i \sin\Omega\, \Delta u_0 \quad (15c)$$

Comparing the two matrices $\boldsymbol{D}_{\text{eop}}$ and $\boldsymbol{D}_{\text{orb}}$, we easily find the relations we were looking for:

$$\Delta(\text{UT1–UTC}) = -(\Delta\Omega + \cos i\, \Delta u_0)/\rho \quad (16a)$$
$$\delta\Delta\epsilon = \cos\Omega\, \Delta i + \sin i \sin\Omega\, \Delta u_0 \quad (16b)$$
$$\delta\Delta\psi \sin\epsilon_0 = -\sin\Omega\, \Delta i + \sin i \cos\Omega\, \Delta u_0 \quad (16c)$$

or vice versa the inverse operation

$$\Delta i = \cos\Omega\, \delta\Delta\epsilon - \sin\Omega\, (\delta\Delta\psi \sin\epsilon_0) \quad (17a)$$
$$\Delta\Omega \tan i = -\sin\Omega\, \delta\Delta\epsilon - \cos\Omega\, (\delta\Delta\psi \sin\epsilon_0) - \tan i\, \rho\, \Delta(\text{UT1–UTC}) \quad (17b)$$
$$\Delta u_0 \sin i = \sin\Omega\, \delta\Delta\epsilon + \cos\Omega\, (\delta\Delta\psi \sin\epsilon_0) \quad (17c)$$

The above equations show how the ERPs and orbital elements are related to each other and makes clear why offsets in nutation and UT1-UTC may not be estimated from GPS (or SLR) data. VLBI (and LLR) measurements are needed to establish these quantities.

From (16) (or (17)) we easily obtain the formulas for the relations between nutation and UT1-UTC rates (or length of day (LOD)) and the first time derivatives of the orbital elements:

$$\dot{(\text{UT1–UTC})} = -\text{LOD} = -(\dot\Omega + \cos i\, \dot u_0)/\rho \quad (18a)$$
$$\Delta\dot\epsilon = \cos\Omega\, \dot i + \sin i \sin\Omega\, \dot u_0 \quad (18b)$$
$$\Delta\dot\psi \sin\epsilon_0 = -\sin\Omega\, \dot i + \sin i \cos\Omega\, \dot u_0 \quad (18c)$$

where LOD is equal to $-\dot{(\text{UT1–UTC})}$ in the absence of leap seconds.

In the Keplerian approximation (two-body problem; bodies with spherically symmetric mass distribution) the orbital elements Ω, i, and u_0 are integration constants and therefore constant in time. This means that there is no problem to estimate nutation rates and UT1-UTC rates (or LOD). This is also true if the orbital elements are perturbed, as long as the perturbing accelerations can be modeled accurately enough over the time interval the rates are estimated for (e.g., for 1–3 days). The interaction between perturbations of the satellite orbits and the nutation rate estimates will be discussed in section 4.2.

In summary, we have shown that it is in principle possible to estimate nutation rates (not nutation offsets, however) from satellite geodetic data. There is no fundamental difference between estimating UT1-UTC rates and nutation rates, and there is no mathematical reason therefore to estimate the former but not the latter.

We have to ask two basic questions, however: (1) what is the frequency range, where nutation rate estimates derived from GPS data may significantly contribute to the estimation of nutation terms ?; (2) what will be the approximate precision of nutation amplitudes estimated from GPS data ?

In order to answer these questions we examine the basic observation equations used to estimate nutation amplitudes from (1) VLBI corrections to the a priori nutation model (e.g., IAU 1980) and (2) nutation rate corrections using GPS. Consider the estimation of the nutation coefficients a_ω and b_ω of one specific nutation period $T = 2\pi/\omega$ from a series of nutation corrections $\Delta\alpha_i$ ($i = 1, 2, \ldots, n$) or nutation rate corrections $\Delta\dot\alpha_i$ ($i = 1, 2, \ldots, n$), where $\Delta\alpha_i$ is either a correction in the nutation in obliquity $\Delta\epsilon$ or in longitude $\Delta\psi \sin\epsilon_0$ (ϵ_0 is the mean obliquity of the ecliptic). We have

$$\Delta\alpha_i = a_\omega \cos(\omega t) + b_\omega \sin(\omega t) \quad (19)$$
$$\Delta\dot\alpha_i = -a_\omega\, \omega \sin(\omega t) + b_\omega\, \omega \cos(\omega t) \quad (20)$$

The first design matrices $\boldsymbol{A_V}$ and $\boldsymbol{A_G}$ in the case of nutation offsets (VLBI) and rates (GPS), respectively, are then given by

$$\boldsymbol{A_V} = \begin{pmatrix} \cos(\omega t_1) & \sin(\omega t_1) \\ \cos(\omega t_2) & \sin(\omega t_2) \\ \vdots & \vdots \\ \cos(\omega t_n) & \sin(\omega t_n) \end{pmatrix} \quad (21)$$

$$\boldsymbol{A_G} = \begin{pmatrix} -\omega \sin(\omega t_1) & \omega \cos(\omega t_1) \\ -\omega \sin(\omega t_2) & \omega \cos(\omega t_2) \\ \vdots & \vdots \\ -\omega \sin(\omega t_n) & \omega \cos(\omega t_n) \end{pmatrix} \quad (22)$$

Assuming equal weight for all nutation observations of one series, we obtain the normal equation matrices N_V and N_G as

$$N_V = A_V^T A_V = \begin{pmatrix} \sum_{i=1}^{n} \cos^2(\omega t_i) & \sum_{i=1}^{n} \cos(\omega t_i)\sin(\omega t_i) \\ \sum_{i=1}^{n} \cos(\omega t_i)\sin(\omega t_i) & \sum_{i=1}^{n} \sin^2(\omega t_i) \end{pmatrix} \quad (23)$$

$$N_G = A_G^T A_G = \omega^2 \begin{pmatrix} \sum_{i=1}^{n} \sin^2(\omega t_i) & -\sum_{i=1}^{n} \cos(\omega t_i)\sin(\omega t_i) \\ -\sum_{i=1}^{n} \cos(\omega t_i)\sin(\omega t_i) & \sum_{i=1}^{n} \cos^2(\omega t_i) \end{pmatrix} \quad (24)$$

If we have a large number of observations n and if the period T considered is much smaller than the lengths of the observation series $T_s = t_n - t_1 \gg T$ and much larger than the typical observation sampling interval $\Delta t \ll T$, we may approximate the sums in (23) and (24) by integrals

$$\sum_{i=1}^{n} \cos^2(\omega t_i) \approx n \frac{1}{2\pi} \int_0^{2\pi} \cos^2(\omega t)\, dt \approx n \frac{1}{2\pi} \int_0^{2\pi} \sin^2(\omega t)\, dt = \frac{n}{2} \quad (25)$$

$$\sum_{i=1}^{n} \sin(\omega t_i)\cos(\omega t_i) \approx n \frac{1}{2\pi} \int_0^{2\pi} \sin(\omega t)\cos(\omega t)\, dt = 0 \quad (26)$$

After the inversion of the normal equation matrices we obtain

$$N_V^{-1} = \begin{pmatrix} \frac{2}{n} & 0 \\ 0 & \frac{2}{n} \end{pmatrix} \quad (27)$$

$$N_G^{-1} = \begin{pmatrix} \frac{2}{n\omega^2} & 0 \\ 0 & \frac{2}{n\omega^2} \end{pmatrix} \quad (28)$$

The formal errors of the coefficients a_ω and b_ω are therefore given by

$$\sigma_V(a_\omega) = \sigma_V(b_\omega) = \sigma_{\Delta\alpha} \sqrt{N^{-1}_{11,V}} = \sigma_{\Delta\alpha} \sqrt{\frac{2}{n}} \quad (29)$$

$$\sigma_G(a_\omega) = \sigma_G(b_\omega) = \sigma_{\Delta\dot\alpha} \sqrt{N^{-1}_{11,G}} = \sigma_{\Delta\dot\alpha} \sqrt{\frac{2}{n}} \frac{1}{\omega} \quad (30)$$

or as a function of the period T

$$\sigma_G(a_T) = \sigma_G(b_T) = \sigma_{\Delta\dot\alpha} \sqrt{\frac{2}{n}} \frac{T}{2\pi} \quad (31)$$

where $\sigma_{\Delta\alpha}$ and $\sigma_{\Delta\dot\alpha}$ are the weighted RMS of the postfit residuals of the nutation corrections $\Delta\alpha$ from VLBI and the nutation rate corrections $\Delta\dot\alpha$ from GPS, respectively.

From (29) we see that all the periods (under the assumptions $T \ll T_s$ and $T \gg \Delta t$ mentioned above) may be estimated with the same formal errors from VLBI nutation series, whereas for the GPS rate series the formal errors of the coefficients grow linearly with the period T. Let us make use of (29) and (31) to compute an estimate of the formal errors to be expected in both cases, using actual numbers for n and σ given in the literature. In the work by *Herring et al.* [1991] we find $n = 798$, $\sigma_{\Delta\alpha} = 0.6$ mas for VLBI and this paper here gives $n = 1281$, $\sigma_{\Delta\dot\alpha} = 0.27$ mas/d for GPS. The resulting formal errors are

$$\sigma_V(a_\omega) \approx 0.030 \text{ mas} \quad (32)$$

$$\sigma_G(a_\omega) \approx 0.0017\,T \text{ mas} \quad (33)$$

The approximate value of $\sigma_V(a_\omega) = 0.03$ mas for VLBI amplitude error estimates is too small by a factor of 2 compared to the value of 0.06 mas (for $\Delta\epsilon$ and $\Delta\psi \sin\epsilon_0$) explicitly given by *Herring et al.* [1991]. This is a consequence of the fact that the $\sigma_{\Delta\alpha}$ quoted above for VLBI has been doubled (from 0.3 to 0.6 mas) to account for unmodeled systematics. In the work by *Souchay et al.* [1995], for example, the weighted RMS of residuals is about 1.2 mas or a factor of 2 larger than the value obtained by *Herring et al.* [1991]. *Charlot et al.* [1995] report formal errors $\sigma_V(a_\omega)$ between 0.03 and 0.05 mas and *Souchay et al.* [1995] mention about 0.016 mas. The most up-to-date values stemming from T.A. Herring (Analysis of the most recent VLBI nutation offset series available at ftp://gemini.gsfc.nasa.gov/pub/solutions/1083_aug97/eop_nutation.1083c; private communication, 1997) (hereinafter referred to as Herring (private communication, 1997)) are $\sigma_{\Delta\alpha} = 0.03$ mas (weighted rms) and $n = 2676$ resulting in $\sigma_V(a_\omega) = 0.008$ mas (in agreement with the actual formal errors obtained in this solution). It is worth mentioning that the VLBI formal errors, without modeling improvements, will decrease only slowly from now on. To reduce the formal errors by a factor $\sqrt{2}$ will require about another 13 years of data (VLBI results improved by almost a factor of 8 from 1991 to 1997!). For GPS, under the same assumptions, that is, without further improvements to the analysis and to the global network, a factor of $\sqrt{2}$ can be gained with another 3 years of data or by adding data prior to March 1994. In addition, it should be pointed out that the GPS orbit quality has improved by a factor of 10 from about 40 cm in 1992 to 4 cm in the beginning of 1998 [*Kouba and Mireault*, 1998].

Figure 1 summarizes the precision of nutation amplitude estimates from VLBI and that expected from GPS over periods from 3 to 40 days. It indicates that GPS could make a useful contribution for periods below 5 to 32 days depending on the duration of the GPS data used and the accuracy assumed for VLBI. The lower limit corresponds to the current duration of GPS data analyzed and the latest VLBI analysis, and the upper limit corresponds to an assumed analysis with twice the duration of GPS data and the Charlot 1995 precision estimate for VLBI. In this paper we will adopt 16 days as the period below which we will examine the accuracy of the GPS amplitude estimates. The break-even point (equal precision for both space techniques) varies somewhere between a period of 5 and 20 days. The simple

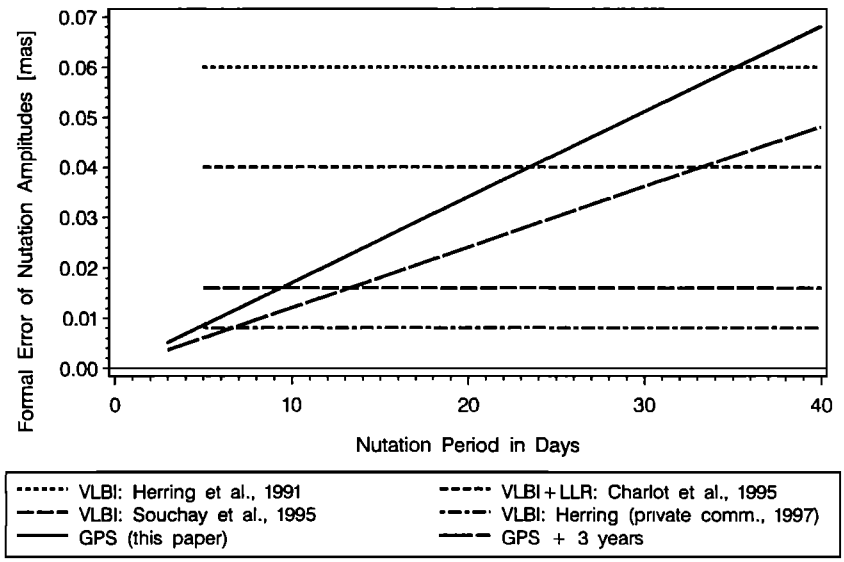

Figure 1. Precision of amplitude estimation from nutation offset corrections (VLBI and LLR) and nutation rate corrections (GPS) derived using a simple variance-covariance analysis.

variance-covariance analysis shows very clearly, that (1) no major contributions to nutation theory may be expected from GPS with current orbit modeling in the low-frequency domain ($T > 16$ days); (2) GPS has a good chance to contribute in the high-frequency range of the nutation spectrum ($T < 16$ days).

The first conclusion was to be expected because of the difficulties of modeling the GPS satellite orbits over more than a few days and the degradation with time of the quasi-inertial frame realized through the equations of motion of the satellites. The second statement, however, may be unexpected in that, for a long time, the access to the rotation axis of the Earth in inertial space was thought to be reserved to VLBI and LLR. At periods of several days we may expect very precise amplitude estimates from the GPS series. This picture is very similar to what we know from the behavior and quality of LOD estimates derived from GPS data [*Gambis*, 1995]. It is clear that when we approach the periods near to the sampling interval (about 5 days in VLBI and 1–3 days in GPS), the relationships (29) and (30) will no longer hold. The same is in principle true for very long periods, but we do not consider such periods here. With a longer time series the horizontal line of the VLBI precision in Figure 1 will be shifted in parallel toward lower values, whereas for GPS the slope of the line will decrease.

3. GPS Data Analysis

3.1. Global Data Set

The GPS data used in this analysis covers a time interval of more than 3 years or 1281 days. It starts in April 1994 (day 112) and ends in November 1997 (day 300). For each day in this interval global solutions were computed using the latest version of the Bernese GPS Software [*Rothacher and Mervart*, 1996], each solution including three consecutive days of data and overlapping with the preceding and the following 3-day solutions (see Figure 2). The reason to generate 3-day solutions (and not, e.g., 1-day solutions) is the strength gained by having 3-day satellite arcs (only one set of initial conditions per satellite for 3 days). The data are from the IGS network shown in Figure 3 and comprise observations from 40 to about 90 globally distributed sites. It can be seen that today the IGS sites are quite homogeneously distributed over the globe (with the exception of the gaps in Africa and Russia, and the dense clusters in Europe and the United States). This polyhedron of sites supplies a very strong reference frame for the determination of Earth orientation parameters. Figure 4 shows the number of sites and the number of phase double-difference observations used in the 3-day solutions. From the steady increase of both quantities we may expect an improvement in the quality of the estimated nutation (and other) parameters over the 3 years considered here. The drastic reduction in the number of observations and stations around day 235 in 1997 is due to a problem at one of the major operational data centers. The lowering of the elevation cutoff angle used in the processing from 20° to 10° in October 1997 resulted in an increase of about 25% in the number of observations.

Instead of having to start from raw data (a very time-consuming procedure) the 3-day solutions we use in this paper could be produced from normal equation systems (only containing site coordinates, Earth orientation parameters,

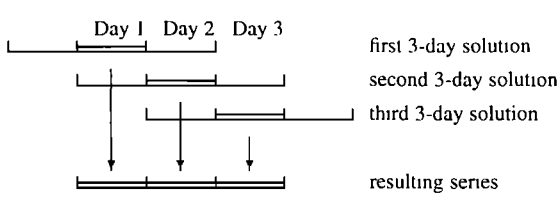

Figure 2. Processing of GPS data at CODE in overlapping 3-day intervals.

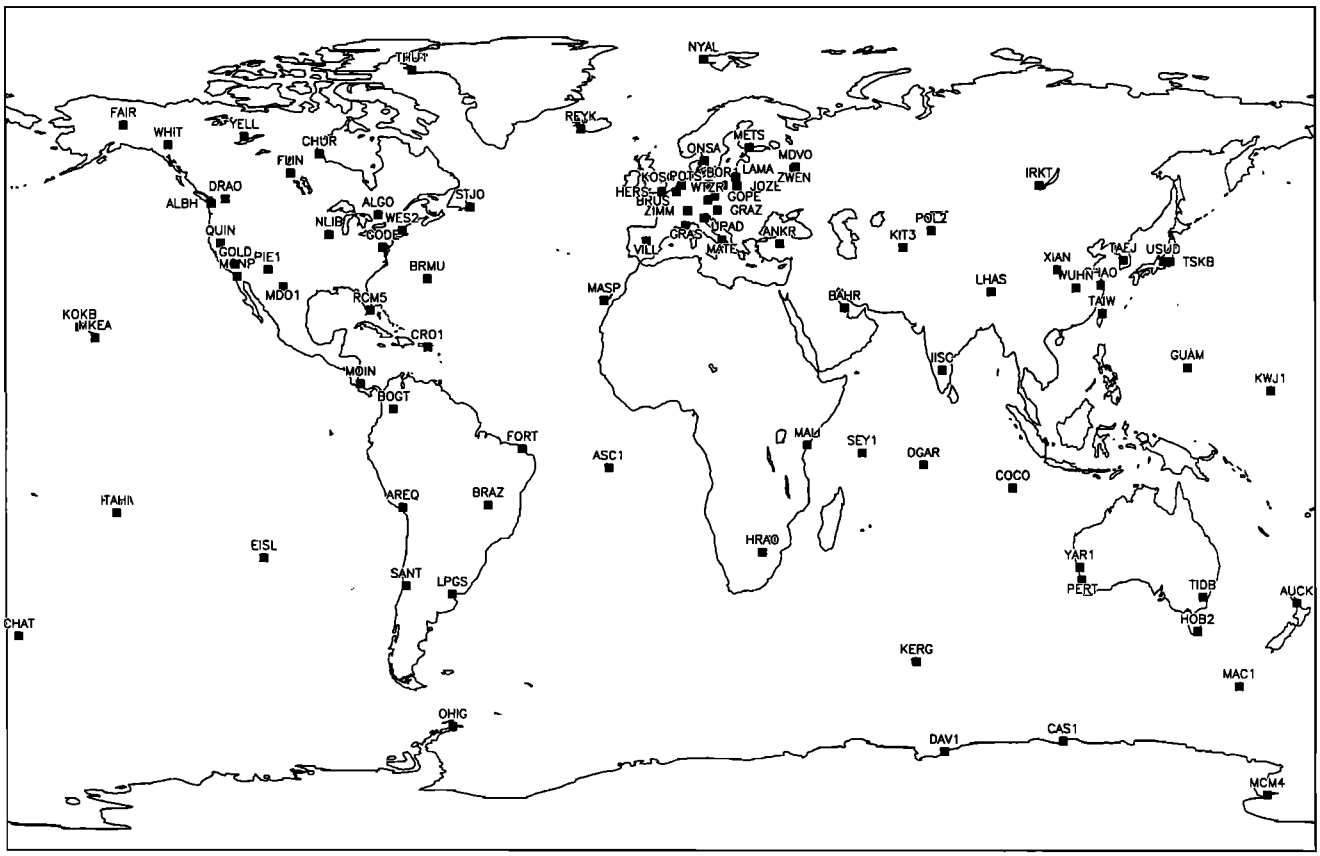

Figure 3. Stations of the global IGS network used by the CODE Analysis Center (status of July 1997).

and geocenter coordinates as unknowns; other parameter types were preeliminated from the system at an earlier stage). These normal equation systems were saved during the routine CODE processing [*Rothacher et al.*, 1997] or during one of the two reprocessing efforts in 1996 [*Botton et al.*, 1997]. The normal equations were generated using a standard least squares algorithm. The combination procedures are described in detail by *Brockmann* [1997].

3.2. Earth Orientation Parameters

When saving the normal equation files much emphasis was put on having a high temporal resolution for the Earth orientation parameters estimated. Therefore offset and rate parameters were set up for each 2-hour interval and for each of the five components of Earth orientation, namely, the x and y pole coordinates, the difference UT1-UTC, and the

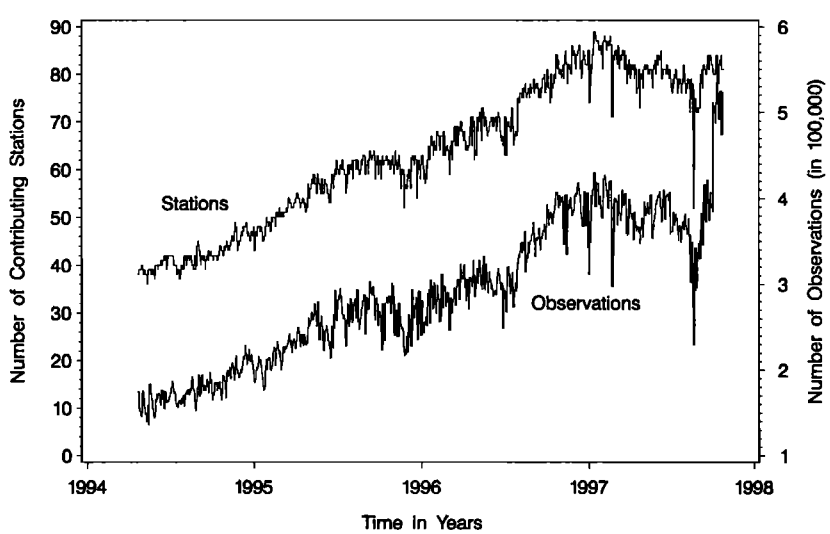

Figure 4. Number of stations and phase double-difference observations included in the 3-day solutions when estimating nutation rates from GPS.

nutation corrections $\delta\Delta\epsilon$ and $\delta\Delta\psi$ in obliquity and longitude. Although the subdaily estimation of all five components does not make sense, they were initially set up the same way out of convenience. An exception is for all days in 1994 (day 112 to day 365), where the binning interval is 1 day (one offset and rate set up per day).

Starting from the 2-hour offset and rate estimates saved in the normal equation systems, it is possible to produce a number of different solution types for the EOPs by either using linear transformations between subsequent parameter sets or by putting a priori constraints on these parameters. Two important features to be mentioned in this context are the forcing of continuity at the interval boundaries and the reduction of the number of parameters per day. Continuity at the interval boundaries was asked for in all the solution types discussed below, that is, the EOPs were always represented as piecewise linear functions. A reduction of the number of parameters, for example, reducing 12 offsets and rates per day to only one offset and rate per day or even to one offset and rate over the entire 3 days, can easily be achieved through linear transformations of the parameters or by appropriate a priori constraints put on the parameters. It should be mentioned that, although offset parameters were set up for all five components, only polar motion (PM), that is, the x and y pole coordinates, may be determined in an absolute sense using GPS data. The first offset of a 3-day solution for UT1-UTC, $\Delta\epsilon$, and $\Delta\psi$ was therefore always constrained to the a priori value (obtained from VLBI).

Three major 3-day solution series, in the following called N3, N1, and S3, were generated for either the entire time period of 3.5 years or for all days since January 1, 1995. Table 1 gives a summary of the most important characteristics of these nutation series estimated from GPS data.

Before discussing why these series were produced, it is essential to know which a priori models were underlying the estimation of the EOP parameters. In the case of nutation the IAU 1980 nutation model [*McCarthy*, 1996; *Seidelmann*, 1982; *Wahr*, 1981] was used as an a priori model for all series and all days. Consequently, all nutation rate estimates $\Delta\dot{\epsilon}$ and $\Delta\dot{\psi}$ are corrections to the IAU 1980 Theory of Nutation. Regarding polar motion and UT, the diurnal and semidiurnal tidal variations of the Earth's rotation were corrected for according to the tidal model given in the IERS Conventions 1996 [*McCarthy*, 1996; *Ray et al.*, 1994] for all solutions from June 30 (day 182) of 1996 onward. This implies that prior to day 182 of 1996, with the exception of the period from day 002–125 in 1995 (which was reprocessed only recently), all solutions of the series N3 and N1 suffer from incomplete modeling of polar motion and UT1 in the subdaily regime (more details about the relations between nutation and subdaily polar motion and UT1 are given by *Sovers et al.* [1993]). For this reason (subdaily variations are not accounted for in series N3 and N1) the series S3 was generated, where polar motion and UT were determined on a 2-hour basis. To avoid singularities, retrograde diurnal polar motion was suppressed using corresponding constraints on the 2-hour polar motion offset and rate parameters. The particular aspect of the series N1 is the higher resolution of the nutation rate estimates (1 day instead of 3), which avoids the smoothing effect to be expected from 3-day solutions.

Table 1. Characterization of the Nutation Series N3 (3-Day Nutation Rates), N1 (1-Day Nutation Rates), and S3 (3-Day Nutation Rates Plus Subdaily PM and UT1-UTC) Estimated From GPS Data (3-Day Solutions)

Series	Time Interval	Number of Days	Interval, hours	
			PM, UT	Nutation
N3	112/1994–300/1997	1281	72	72
N1	112/1994–300/1997	1281	72	24
S3	002/1995–300/1997	1030	2	72

3.3. Orbit Model and Parameters

The fact that most of the solutions presented here are based on the routine products of CODE may explain the inhomogeneity of the series from the point of view of orbit modeling and parameterization. In order to improve the routine solutions and products, a continuing development of software and strategies is necessary. With such changes CODE tries to maintain a high-quality level for the "routine" products. The time series of solutions, however, become inhomogeneous and difficult to interpret due to such modifications. Unfortunately, it is not feasible yet to reprocess a few years of data "from scratch" each time a major modification is made, due to the amount of data involved. In this section we focus on the aspects of orbit modeling that are relevant to understanding our nutation series.

In general, the orbit of each satellite over 3 days was represented by one set of initial conditions (position and velocity vector at the start of the interval), by one set of radiation pressure parameters (more details will be given below), and by pseudo-stochastic pulses (small changes in the satellite's velocity) [*Beutler et al.*, 1996b]. Such pulses were introduced in the along-track and radial direction every 12 hours, that is, 5 times in a 3-day interval. They were constrained (to zero) with an a priori variance of $(10^{-5}$ m/s$)^2$ and $(10^{-6}$ m/s$)^2$ for the along-track and radial component, respectively. Before January 1995, pseudo-stochastic pulses were set up for eclipsing satellites only, and thereafter for all satellites. For satellites that were difficult to model on specific days (even with the estimation of pseudo-stochastic pulses), the 3-day arc was split up at the day boundaries into 2 or even 3 arcs by estimating additional sets of initial conditions and radiation pressure parameters.

The radiation pressure model in use at CODE in its general form is defined by *Beutler et al.* [1994b]:

$$\mathbf{a}_{\mathrm{rpr}} = \mathbf{a}_{\mathrm{ROCK}} + D(u)\,\mathbf{e}_{\mathrm{D}} + Y(u)\,\mathbf{e}_{\mathrm{Y}} + X(u)\,\mathbf{e}_{\mathrm{X}} \qquad (34)$$

where

$$\begin{aligned} D(u) &= a_{D0} + a_{DC}\cos(u) + a_{DS}\sin(u) \\ Y(u) &= a_{Y0} + a_{YC}\cos(u) + a_{YS}\sin(u) \\ X(u) &= a_{X0} + a_{XC}\cos(u) + a_{XS}\sin(u) \end{aligned} \qquad (35)$$

and where a_{rpr} denotes the total acceleration due to solar radiation pressure, a_{ROCK} the acceleration according to the ROCK4/42 models [*Fliegel et al.*, 1992]. Variables e_D and e_Y are unit vectors in the direction Sun-satellite and in the direction of the solar panel axis, and e_X forms a right-hand system with e_D and e_Y. Variable u is the argument of latitude of the satellite and a_{D0}, a_{Y0}, a_{X0}, a_{DC}, ..., a_{XS} are the nine parameters of the model. The coefficients a_{D0} and a_{Y0} are the two parameters of the so-called "classical" model: the direct radiation pressure coefficient and the Y bias.

Whereas only the two classical radiation pressure parameters were determined until day 273, 1996, after this date the number of parameters was increased to five: the three constant terms (a_{D0}, a_{Y0}, and a_{X0}) and the periodic terms in X direction (a_{XC} and a_{XS}). We will refer to these two orbit models as the "old" and the "new" orbit model in the following. To estimate even more of the nine parameters would lead to high correlations between some of these parameters and the EOPs (in particular, UT1-UTC and nutation rates and the geocenter coordinates; see section 4.2). The selection of these very five parameters was mainly based on an optimization of the quality of the orbits and the quality of the UT1-UTC rate estimates [*Springer et al.*, 1996, 1998]. The quality of the nutation rate estimates was not a criterion at this point in time.

To complete the description of the orbit modeling, let us mention that small changes in the force field (e.g., improved Earth tide model, use of the Jet Propulsion Laboratory (JPL) Planetary Ephemeris DE200, etc.) took place in July and October 1996 (see *Rothacher et al.* [1997] for more details). In particular, ocean tide forces on the satellites have been implemented on day 273, 1996, according to the CSR 3.0 ocean tide height model [*McCarthy*, 1996]. From what we know about the behavior of the UT1-UTC rates, we may expect that these modifications mainly result in a change of the (more or less) constant bias in the nutation rates and thus only affect the long-term variations not accessible to GPS anyway. An exception might be ocean tide model errors in the orbits. The size of such orbit errors might be of the order of 1 mm for GPS satellites [*McCarthy*, 1996]. However, due to the fact that the nutation rate estimates are average values over 3 days (N3 and S3) or one day (N1), biases in the orbits with periods around 1 day will be reduced to almost zero in the 3-day nutation rates and by about 30% in the 1-day nutation rates (see dashed line in Figure 9, section 5.2, with a ratio of 0.3 and 1.0, respectively, between period and estimation interval). A further reduction of, possibly, up to $\sqrt{6}$ could result from the six orbital planes present in the GPS, so that no significant biases in the nutation rate estimates may be expected from this error source.

The major improvements in the orbit quality were certainly achieved by allowing for pseudo-stochastic pulses for all satellites and by the switch to five radiation pressure parameters. The effect of these changes on the nutation estimates will be discussed in section 5.

3.4. Other Parameters Estimated

Together with the EOPs and orbit parameters discussed in the last two sections, other parameter types were estimated simultaneously: site coordinates, site-specific troposphere zenith delays, initial phase ambiguities, geocenter coordinates, and satellite antenna offsets. These parameters were treated in exactly the same way in all of the three series N3, N1, and S3.

Site coordinates were set up for all sites. The global reference frame was realized by heavily constraining 12 well-distributed sites to their International Terrestrial Reference Frame 1994 (ITRF94) coordinates (converting the coordinates to the actual epoch using the ITRF94 velocities [*Boucher et al.*, 1996]. The other sites were freely estimated. The site displacements due to solid Earth tides were modeled according to the IERS Conventions 1996 [*McCarthy*, 1996], but ocean loading was not corrected for. Because the nutation rates were estimated over a time interval of at least one full day and because the ocean tides are largely radial, the unmodeled ocean loading effects should not affect the nutation rates too much, especially with the good global distribution of sites. *Herring and Dong* [1994] discuss the effects of tides on VLBI solutions; *Watkins and Eanes* [1994] discuss those on SLR solutions.

For every 6-hour interval a troposphere zenith delay parameter was determined for each site. The mapping function derived by *Saastamoinen* [1971] was used to map the zenith delays to the actual satellite elevation angle.

Since January 1995, 80–90% of the initial phase ambiguities were resolved to integer numbers for all baselines shorter than 2000 km using a strategy called Quasi Ionosphere-Free described by *Mervart* [1995]. For baselines longer than 2000 km, no ambiguity resolution was performed. On the average about 50% of the total number of ambiguities could be resolved.

4. Correlation Between EOPs and Orbit Parameters

4.1. Correlation Between EOPs

When aiming at an almost instantaneous estimation of EOPs, at the most three independent Earth rotation parameters may be estimated, namely, the three Eulerian angles defining the net transformation matrix between the inertial and the Earth-fixed reference frame. When estimating more parameters (e.g., polar motion in x and y, UT1-UTC, $\Delta\epsilon$, and $\Delta\psi$) these parameters will be linearly dependent or highly correlated. Uniqueness is achieved by forbidding prograde diurnal terms in nutation and retrograde diurnal terms in polar motion. In practice the correlations actually occurring between the five EOPs depend mainly on the binning intervals used. Table 2 lists the correlations between the EOPs we have set up for the main solution type N3 (see Table 1). Most of the parameter types are almost uncorrelated. Significant correlations exist, on the other hand, between the nuta-

Table 2. Correlations Between the EOPs Estimated in a 3-Day Solution of Type N3

Parameter	$\dot{x}$	y	$\dot{y}$	UT1–UTC	$\Delta\dot{\epsilon}$	$\Delta\dot{\psi}$
x	-0.04	-0.11	0.04	0.01	0.01	-0.06
$\dot{x}$	.	0.01	-0.04	-0.03	-0.06	0.03
y	.	.	-0.03	-0.02	0.04	0.01
$\dot{y}$	.	.	.	0.04	-0.01	-0.03
UT1–UTC	.	.	.	.	0.35	-0.39
$\Delta\dot{\epsilon}$	.	.	.	.	.	-0.30

tion rates and the UT1-UTC rate. The simultaneous estimation of the above parameters is therefore not really critical. The picture is almost the same when looking at solution type N1, but the highest correlations drop to about 0.25 (due to the higher time resolution of the nutation rate estimates). For solution S3 the correlations between nutation rates and UT1-UTC rate are almost zero. The estimation of subdaily polar motion and LOD gives rise to periodically changing correlations during the day between the 2-hour pole values and the nutation rate parameters with amplitudes between 0.5 and 0.8 indicating that, in general, even when suppressing the retrograde diurnal terms, polar motion with subdaily resolution should not be estimated together with nutation rates. The formal errors of the nutation rate estimates grow considerably for solution type N1 and S3 compared to solution N3 as we will see in section 5.

4.2. Correlation Between Orbit Parameters and ERPs

We now examine equations (18) more closely, because they are crucial for the understanding of correlations between the EOPs and orbital parameters. According to (18a), the LOD estimates are related to changes in the orbital nodes and changes of the argument of latitude u_0. A drift in the node Ω, common to all satellites (e.g., produced by a slightly wrong Earth potential coefficient C_{20}), will directly propagate into the LOD estimates. This is also the case for a common drift in u_0, because the inclination i is almost the same for all GPS satellites. The larger the inclination of the orbits are, the less LOD values are affected by drifts in u_0. The worst case, indeed, results for satellite orbits with an inclination near zero degrees, because all along-track errors and errors in the nodes would directly propagate into the LOD series. For GPS satellites with $i \approx 55^{\circ}$ drifts in u_0 propagate into LOD with the factor $\cos i \approx 0.57$ (0.42 for the Global Navigation Satellite System (GLONASS) with $i \approx 65^{\circ}$). In view of the known fact that the along-track component is the most difficult to model, we may expect a considerable impact of unmodeled drifts in u_0 on the LOD estimates.

For the estimation of the nutation rates $\Delta\dot{\epsilon}$ and $\Delta\dot{\psi}$, changes in u_0 from unmodeled perturbation forces are even more critical ($\sin i \approx 0.82$), but part of the effect may average out because of the different node values for different orbital planes. The nutation rates are affected in a similar way by changes of the orbit inclination i (see (18b) and (18c)).

We thus see that all perturbing accelerations leading to temporal changes of the orbital elements Ω, i, and u_0 are of crucial importance when estimating nutation rates and LOD. Those dynamical orbit parameters (parameters of the force field), that have an impact on the orientation of the orbital plane, are therefore expected to be strongly correlated (according to (18)) with nutation rate estimates. First-order perturbation theory in the Keplerian elements [see, e.g., *Beutler*, 1991], simplified for the case of almost circular orbits ($e \approx 0$), links the time derivatives of the Keplerian elements with the perturbing accelerations ($\boldsymbol{R}$, $\boldsymbol{S}$, $\boldsymbol{W}$), where $\boldsymbol{R}$, $\boldsymbol{S}$, and $\boldsymbol{W}$ are the radial, the tangential, and the out-of-plane components of the perturbing acceleration. The resulting (simplified) equations for the semimajor axis a, the eccentricity e, the inclination i, the ascending node Ω, and the argument of latitude u_0 at epoch t_0 are

$$\dot{a} = \frac{2}{n}\boldsymbol{S} \tag{36a}$$

$$\dot{e} = \frac{1}{n\,a}(\sin u\,\boldsymbol{R} + 2\cos u\,\boldsymbol{S}) \tag{36b}$$

$$\dot{i} = \frac{\cos u}{n\,a}\boldsymbol{W} \tag{36c}$$

$$\dot{\Omega} = \frac{\sin u}{n\,a\,\sin i}\boldsymbol{W} \tag{36d}$$

$$\dot{u_0} = -\frac{2}{n\,a}\boldsymbol{R} - \cos i\,\dot{\Omega} + \frac{3}{2}\frac{n}{a}(t - t_0)\,\dot{a} \tag{36e}$$

where n is the mean motion of the satellite.

By substituting (36) into (18) we get relationships between the acceleration components $\boldsymbol{R}$, $\boldsymbol{S}$, $\boldsymbol{W}$, and the nutation rates. Starting from such equations, it is possible to compute (by numerical or analytical integration) the net effect of an arbitrary unmodeled perturbing acceleration on the nutation rate estimates. Changes in Ω and i, for example, are (according to (36c) and (36d)) uniquely produced by unmodeled accelerations in the out-of-plane direction $\boldsymbol{W}$, whereas (see (36e)) all three acceleration components $\boldsymbol{R}$, $\boldsymbol{S}$, and $\boldsymbol{W}$ contribute to changes in u_0 and thus to biases in the nutation estimates.

The most critical part of the force model for GPS satellites is the acceleration caused by solar radiation pressure. When we express the perturbation due to radiation pressure parameters in the $\boldsymbol{RSW}$ frame, we may compute the net effect of the radiation pressure parameters on the orbital elements and, consequently, on the nutation rates. Such an analysis was performed by *Rothacher et al.* [1995] for the direct radiation pressure parameter a_{D0} and the Y bias a_{Y0} (see (34) and (35)), and it might be extended to comprise the other estimated radiation pressure parameters in (35). The results of such an analysis clearly show that the dominant effects to be expected from radiation pressure are either short-period perturbations (with the revolution period of the satellites) or long-term variations with typically annual and semiannual periods (orientation of the orbital planes relative to the direction to the Sun). Both types of variations are, fortunately, not critical for the nutation periods between a few days and

about 16 days that are accessible to GPS with a reasonable accuracy. Large systematic effects in the nutation rates are to be expected at long periods, especially at semiannual and annual periods.

As we will see from the formal errors of the estimated nutation rates in the next section, a significant correlation exists between the radiation pressure parameter a_{X0} and the nutation rates. This means that the nutation estimates after day 273, 1996, where we started to estimate a_{X0} (and periodic terms in the X direction), are less precisely determined on the one hand, but systematic biases due to orbit modeling problems may be considerably reduced on the other hand. The orbit model quality is definitely the limiting factor in the determination of nutation rates from GPS. A major advantage of VLBI is that its inertial coordinate frame is much better defined by the almost stationary quasars. But even for VLBI there can be motions of the brightest point in some quasars [see, e.g., *Bartel et al.*, 1986].

5. Analysis of the Nutation Rate Series

5.1. Nutation Rate Series From GPS

The three nutation rate series, obtained from processing of the global GPS data as defined in Table 1, are shown in Figure 5. They are the starting point for the estimation of nutation amplitudes. In all three series we see nutation rate corrections with respect to the IAU 1980 model of up to about 1 mas/d. Comparing the IAU 1980 nutation theory (IAU80) to more recent and improved models (e.g., the model defined in the IERS Conventions 1996 (IERS96) [*McCarthy*,

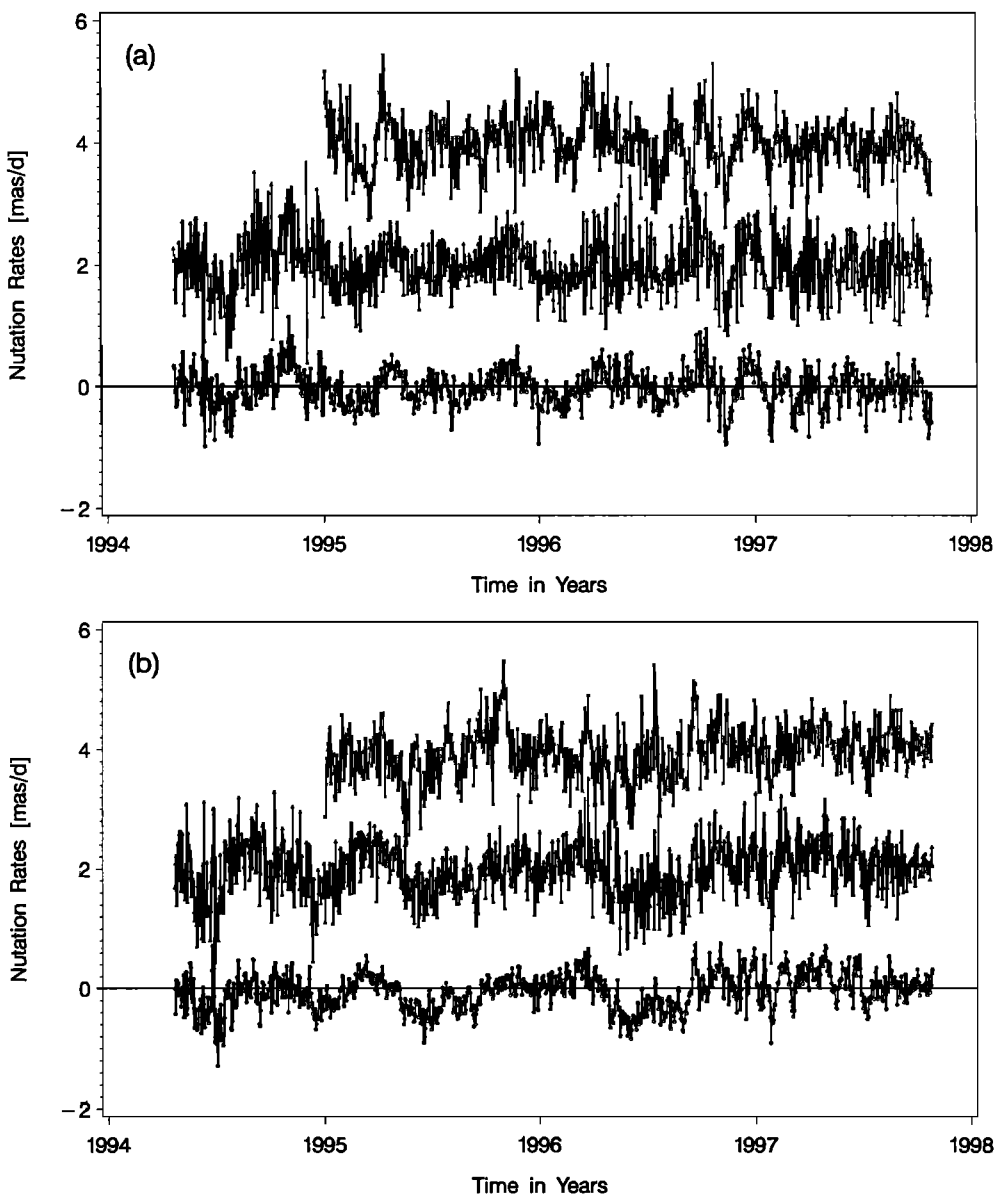

Figure 5. Nutation rates estimated from GPS data between day 112/1994 and day 300/1997 for the three solution types defined in Table 1 (circles, N3; triangles, N1; crosses, S3). Solutions N1 and S3 are offset by +2 mas/d and +4 mas/d, respectively. (a) Rate estimates in $\Delta\epsilon$ and (b) rate estimates in $\Delta\psi \sin \epsilon_0$.

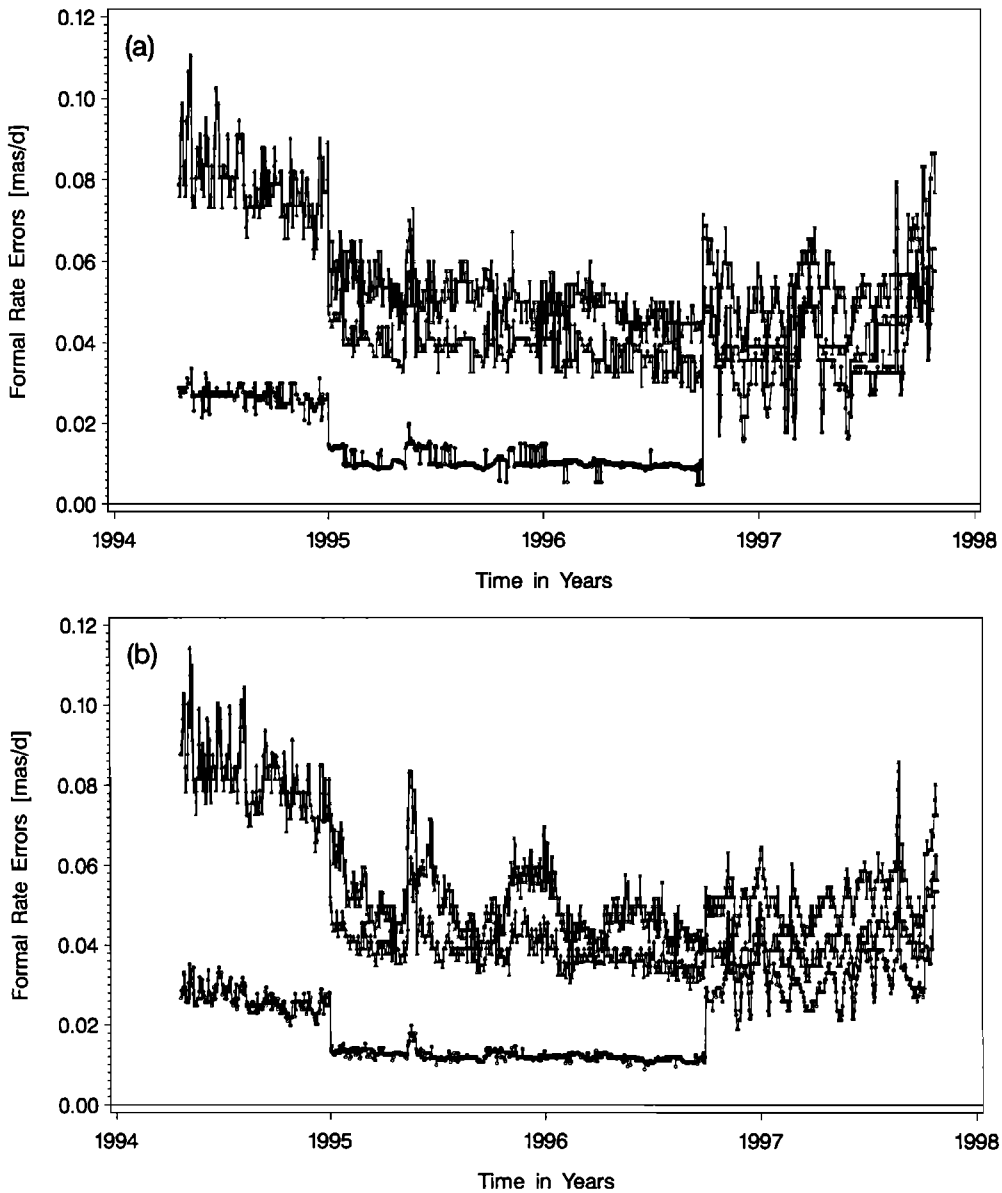

Figure 6. A posteriori formal errors of the nutation rates estimated from GPS data from day 112/1994 to day 300/1997 for the three solution types defined in Table 1 (circles, N3; triangles, N1; crosses, S3). (a) Formal errors of rate estimates in $\Delta\epsilon$ and (b) formal errors of rate estimates in $\Delta\psi \sin \epsilon_0$.

1996]), the differences in the nutation rates are expected to be of the order of 0.25 mas/d over the time interval considered here. This indicates that the GPS series exhibit a noise level which is quite large compared to the expected signal. The N3 series shows the smallest scatter of the three series, smaller than the N1 series due to the estimation of only one nutation rate over 3 days in N3. The scatter of the series S3 is increased because of correlations with the subdaily ERP estimates. Some systematic features (e.g., around the beginning of 1997) are visible in all three series and are probably due to orbit modeling deficiencies, although a coincidence with, for example, eclipse seasons could not be found. The presence of semiannual variations is evident in the obliquity component of the N3 series. Figure 6 gives an impression of the a posteriori formal errors of the nutation rate estimates coming from the global least squares adjustments. Quite a few interesting features are visible in these figures: (1) there is a significant decrease in the formal errors at the beginning of 1995 due to ambiguity fixing after January 2, 1995 (reprocessing); (2) the change of the orbit model in October 1996 caused the formal errors to grow (by a factor of about 2–3 for solution type N3; chi-square per degree of freedom decreases from 1.8 to 1.1), a clear evidence for correlations between the newly added orbit parameters and the nutation rate estimates. A degradation of the quality of the nutation series might be the consequence after this date; (3) before the orbit model change, the series N3 and N1 differ by about a factor of 3 in the formal errors. This is in good agreement with the factor 3.3 expected from theory when estimating three rates (solution N1) instead of one (solution N3) over an interval of 3 days. After the orbit model change the formal errors are dominated by the effects of correlations

with orbital parameters; (4) the formal errors of the S3 series are much higher than those of the N3 series and show large variations in longitude also during the period where the old, "classical" orbit model was used. The simultaneous estimation of subdaily ERPs, although possible in principle, should be avoided. This solution type was computed only, because no model for subdaily polar motion and LOD variations was used for a considerable part of the entire series.

The use of 3-day solutions has a considerable effect on the formal errors of the nutation rate parameters: rates estimated from only one day of data (instead of three) will formally be less accurately determined by a factor of 5.1 (decrease of the formal rate errors with $\Delta T^{-3/2}$, where ΔT is the estimation interval). The estimation of only one rate over 3 days leads, however, to a smoothing at short periods that we will be looking at in more detail below.

As an illustration, we include Figure 7 with the complete amplitude spectra for both nutation components, $\Delta\epsilon$ and $\Delta\psi \sin\epsilon_0$, generated from the rate estimates of the N3 series. The rate amplitudes are corrections with respect to the IAU 1980 model. The actual nutation amplitude a_T at period T may be computed from the rate amplitude a_{rate} given in Figure 7 by

$$a_T = a_{\text{rate}} \frac{T}{2\pi} \tag{37}$$

This relation implies that the actual amplitudes are rapidly growing in size with the length of the period. This has to be expected when looking at a spectrum of rate and not offset estimates. The prominent semiannual peak in the spectra has an actual amplitude of about 4 mas and is a consequence of the correlation between solar radiation pressure parameters (which also show variations with semiannual and annual periods) and the nutation parameters. The interesting part of the spectrum starts below periods of about 20 days. To give a first impression of the type of signal contained in the GPS rate series this section of the spectrum is shown in Figure 8a. To produce this figure the spectrum has been converted from rate amplitudes to amplitudes according to (37) and from $\Delta\epsilon$ and $\Delta\psi \sin\epsilon_0$ to amplitudes a^+ and a^- of circular nutation according to (40) (defined in the next section). It is compared to the spectrum (shown in Figure 8b) to be expected from the differences between the a priori model used (IAU80) and the improved IERS96 model. In principle, the spectral lines in Figure 8b would be delta functions, but the spectrum has been produced from 1-day values (same sampling as N3 series) resulting in peaks with finite bandwidth. Many of the deficiencies of the IAU 1980 theory shown in Figure 8b (e.g., for the 13.66-day prograde and the 5.64-day retrograde term), that were discovered by VLBI about a decade ago, are clearly seen by GPS as well. At high fre-

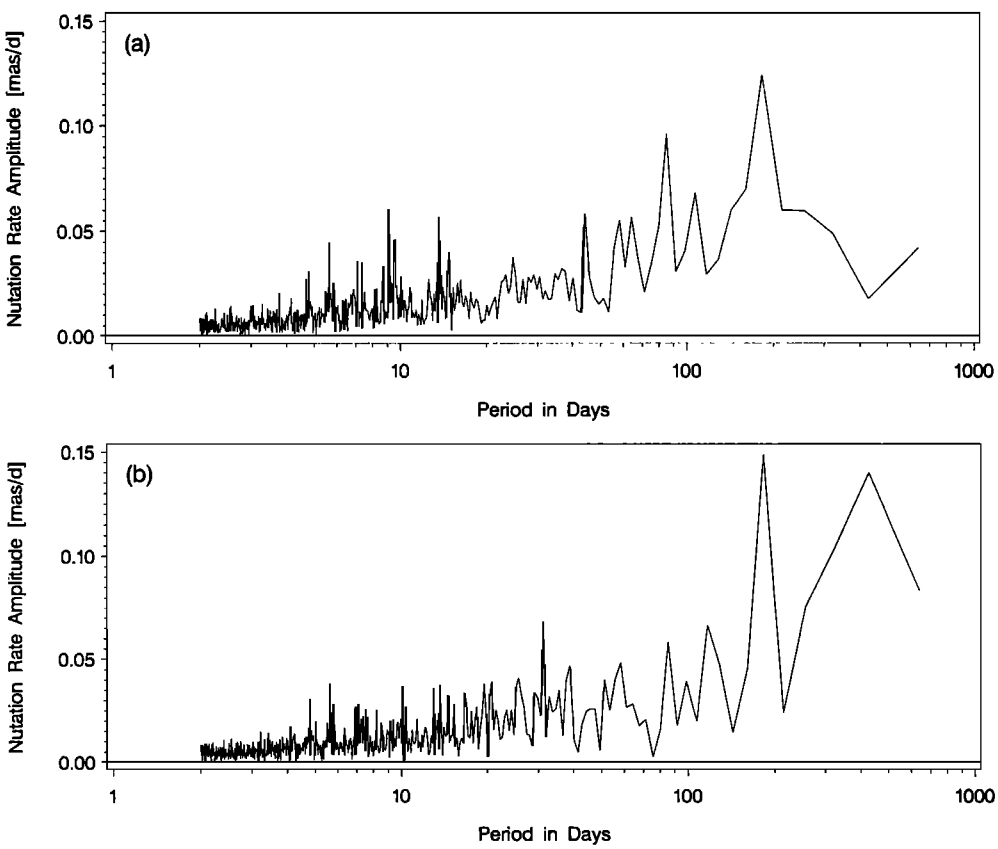

Figure 7. Amplitude spectra generated from series N3 of nutation rates. To obtain the actual nutation amplitudes, the rate amplitudes in mas/d have to be multiplied by the factor period/(2π). The spectrum shows the corrections relative to the IAU 1980 theory, which was used as an a priori model. (a) Spectrum of nutation rates in $\Delta\epsilon$ and (b) spectrum of nutation rates in $\Delta\psi \sin\epsilon_0$.

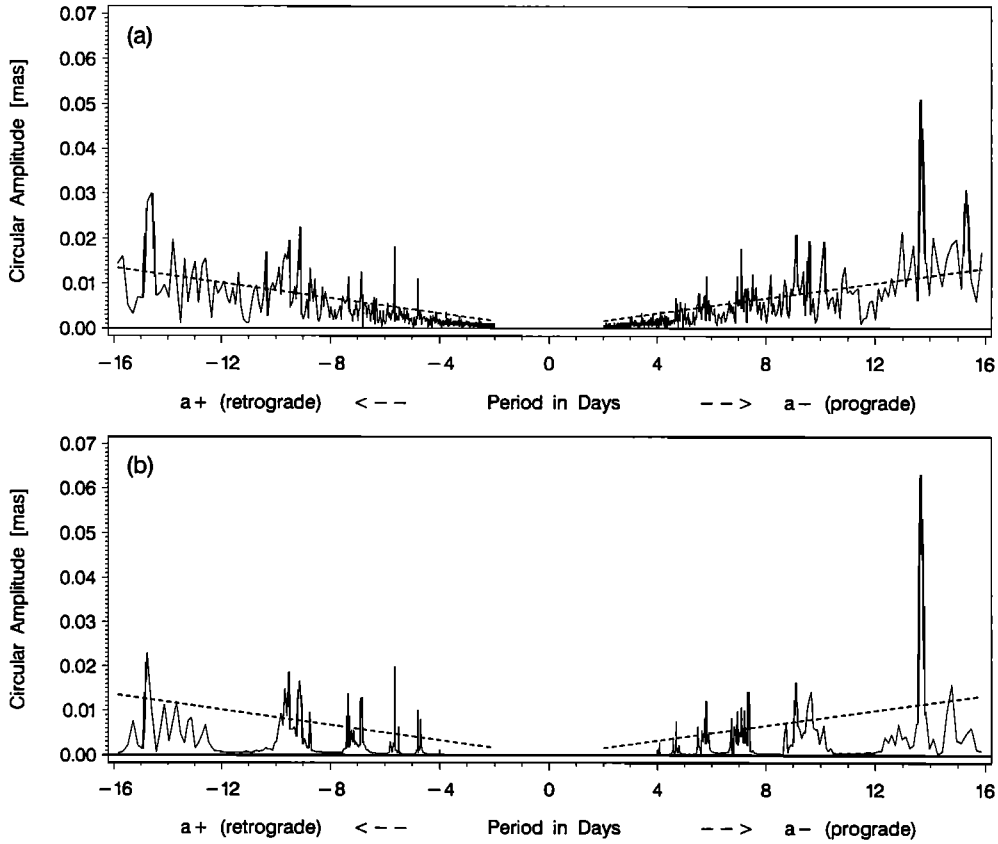

Figure 8. Spectrum of circular nutation amplitudes (see (40)) at low periods generated from (a) the N3 series of GPS nutation rates relative to the IAU80 model, converted to actual nutation amplitudes using (37), and (b) the differences between the IERS96 and the IAU80 model. The dashed lines indicate the 1σ uncertainties of the amplitudes as expected according to (33) (and (40)).

quencies the major deficiencies in the IAU80 model are a result of the truncation of the coefficients to 0.1 mas. There are some spectral lines in Figure 8a that are not present in Figure 8b and these will be discussed later.

The dashed lines in Figures 8 give the expected 1σ uncertainties of the amplitude estimation according to the relationship (33) (divided by a factor of 2 to account for the conversion to circular components of nutation) and indicate what nutation signal should be detectable with GPS.

5.2. Estimation of Nutation Amplitudes

To avoid problems caused by the truncation of the IAU 1980 series, the rate values according to the IAU 1980 theory were added to the rate corrections (with respect to the IAU 1980 model) estimated from GPS to obtain a series of total nutation rates. The more accurate IERS 1996 (IERS96) nutation model including the planetary nutation terms [*McCarthy*, 1996] was then used as a reference model. Nutation corrections were estimated for a number n of selected periods relative to this reference model. The correction $\delta\Delta\epsilon$ and $\delta\Delta\psi$ in the nutation angles were thereby represented by

$$\delta\Delta\epsilon(t) = \sum_{j=1}^{n} (\delta\epsilon_{rj}\cos\theta_j(t) + \delta\epsilon_{ij}\sin\theta_j(t)) \quad (38a)$$

$$\delta\Delta\psi(t) = \sum_{j=1}^{n} (\delta\psi_{rj}\sin\theta_j(t) + \delta\psi_{ij}\cos\theta_j(t)) \quad (38b)$$

with θ_j denoting a combination of the fundamental nutation arguments, namely,

$$\theta_j = \sum_{i=1}^{5} N_{ij}F_i \quad (39)$$

where N_{ij} are integer multipliers of the fundamental arguments $F_i \in \{l, l', F, D, \Omega\}$, also called Delaunay variables, and the angular frequency of the term j is given by $\omega := d\theta_j/dt$.

An alternative representation uses the circular components of nutation a^+_{rj}, a^-_{rj}, a^+_{ij}, and a^-_{ij}, which are related to the nutation coefficients in obliquity and longitude by

$$a^+_{rj} = -(\delta\epsilon_{rj} + \delta\psi_{rj}\sin\epsilon_0)/2 \quad (40a)$$

$$a^-_{rj} = -(\delta\epsilon_{rj} - \delta\psi_{rj}\sin\epsilon_0)/2 \quad (40b)$$

$$a^+_{ij} = -(\delta\epsilon_{ij} - \delta\psi_{ij}\sin\epsilon_0)/2 \quad (40c)$$

$$a^-_{ij} = +(\delta\epsilon_{ij} + \delta\psi_{ij}\sin\epsilon_0)/2 \quad (40d)$$

We follow the conventions adopted by *Herring et al.* [1991]. More details about the interpretation of the circular nutation

components may be found there. We will make use of the circular nutation components in the result section.

The determination of the coefficients $\delta\epsilon_{rj}$, $\delta\epsilon_{ij}$, $\delta\psi_{rj}$, and $\delta\psi_{ij}$ was performed using a least squares algorithm according to the basic formulas (equation (20) and following) developed in section 2 introducing the rate estimates from the GPS analysis as pseudo-observations. In this procedure the rate observations may or may not be weighted according to the formal errors of Figure 6. The corresponding results will be called weighted and unweighted. It also proved to be important to allow for an offset and drift over the entire nutation rate series, that is, to estimate a nutation drift and drift rate to remove long-term variations.

The set of nutation periods for which we decided to estimate coefficients was selected according to the following criteria: (1) the period has to be smaller than 16 days according to the conclusions drawn in section 2 (see Figure 1); (2) the amplitude of the term given by the IERS96 model should be larger than the expected formal error in Figure 1; (3) the periods of two estimated terms should be sufficiently separated to avoid significant correlations between the coefficients. The term with the larger amplitude is chosen, if two or more periods are too close to each other.

Criterion (3) is met by requiring that the phases of the two neighboring periods T_0 and $T_0 + \Delta T$ differ by at least 2π after a time interval equal to the length T_s of the series considered, or

$$\frac{2\pi}{T_0} T_s - \frac{2\pi}{T_0 + \Delta T} T_s \geq 2\pi \tag{41}$$

and thus in first-order approximation,

$$\Delta T \geq \frac{T_0^2}{T_s} \tag{42}$$

Our time series have a length of $T_s = 1281$ days and, according to (42), periods around 5 days have to differ by $\Delta T \approx 0.02$ day, periods around 15 days by $\Delta T \approx 0.18$ day. The set of 34 nutation periods resulting from the above considerations is listed in Table 4 together with the multipliers N_i.

One more effect should be considered when estimating corrections to nutation terms from rate (or offset) pseudo-observations. Let us assume that we estimate rate parameters (GPS) or offset parameters (VLBI) with a time resolution of τ days from the original data (e.g., one rate estimate over $\tau = 3$ days for solution N3). In a second step we then use these estimated rate values (GPS) or offset values (VLBI) to determine nutation amplitudes. What happens if the nutation period T of interest is not much larger than the time interval τ? It is clear that the nutation signal with a period T and an amplitude A originally present in the observations will be damped and we will only recover a fraction of the original amplitude. Figure 9 shows the fraction of the original amplitude we recover as a function of the ratio T/τ. In the case of the GPS series N3 with rate values with a time resolution of $\tau = 3$ days, the nutation amplitudes estimated at a period T of, for example, 6 days (ratio $T/\tau = 2$) will be underestimated by about 25%. Even at periods of about 13 days, a systematic reduction of about 5% of the estimated amplitudes compared to the actual amplitudes still occurs. For solution type N1 with a 1-day resolution the situation is more favorable and we reach the 5% reduction level already for periods above 4 days. From Figure 9 we also learn that the situation is worse, if we are working with nutation offsets to estimate amplitudes. For VLBI offset estimates stemming from experiments of typically 24 hours the attenuation is at a level of 10% for periods around 4 days (amplitude loss for VLBI at high frequencies is also discussed by *Herring and Dong* [1994]). There is no shift in phase to be expected from this smoothing mechanism.

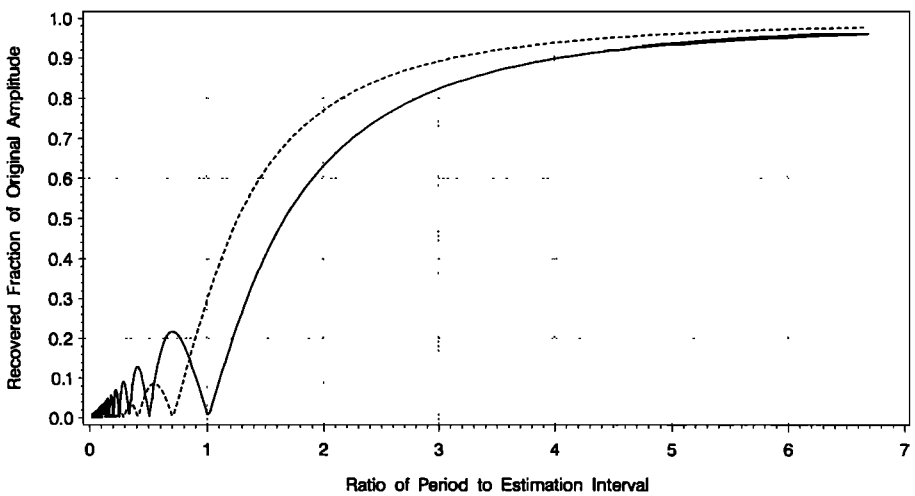

Figure 9. Fraction of the amplitude of the original nutation signal recovered as a function of the ratio between the nutation period T considered and the time resolution τ of the rate (GPS) or offset (VLBI) values determined from the original data. Solid line, amplitude estimated from offsets; dashed line, amplitude estimated from drifts.

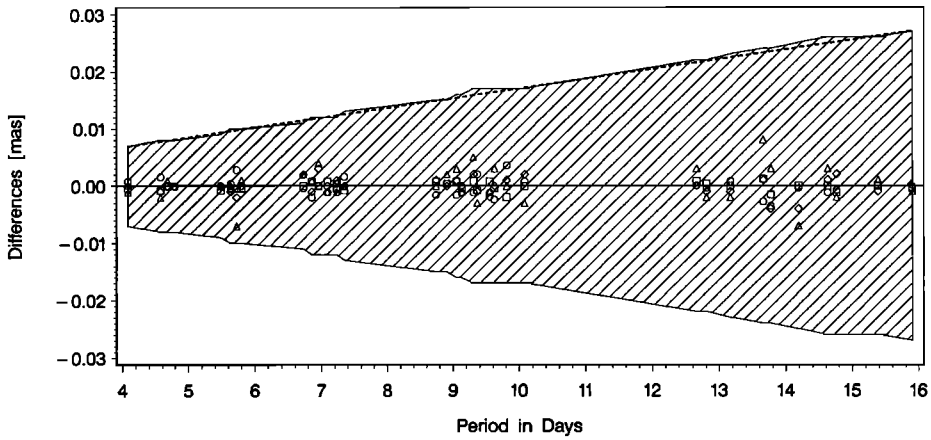

Figure 10. Differences in the estimated nutation coefficients (according to Table 4) due to a change of the a priori nutation model from IERS96 to SKV972. The solutions were produced from the N3 series without weighting the rate values. The shaded area gives the GPS 1σ uncertainties of the estimates. Dashed line, approximate precision expected according to (33), section 2; solid line, 1σ error band; circles, $\Delta\psi \sin\epsilon_0$ sine terms; squares, $\Delta\psi \sin\epsilon_0$ cosine terms; diamonds, $\Delta\epsilon$ sine terms; triangles, $\Delta\epsilon$ cosine terms.

The curves depicted in Figure 9 have been computed using simulation techniques. An analytical approach leads to transcendental equations in the case of rate estimates. It is interesting to note that Figure 9 also helps to interpret results where the signal period is equal to or smaller than the time resolution of the pseudo-observations. Unmodeled diurnal UT1 variations, as an example, will bias daily LOD estimates with about 30% of their original amplitude (ratio $T/\tau = 1$). The effect of semidiurnal variations will propagate with approximately 10% into daily estimates. A variety of other aliasing mechanisms may be looked at in this way. The values given in Figure 9 could be used to correct amplitudes for the smoothing effect.

It is clear that the damping effects can easily be avoided if the nutation amplitude corrections are estimated directly from the original (GPS or VLBI) observations. This approach has been followed by, for example, *Herring et al.* [1991] when estimating nutation corrections from VLBI data. Because, internally, we have set up the nutation parameters with a 2-hour resolution, coefficients of nutation periods could be estimated directly from the 2-hour parameters by means of a linear transformation between the nutation rate parameters and the nutation amplitude coefficients. We plan to perform such an analysis in the future.

Nutation coefficients were determined using the procedure discussed above based on all three nutation series (N3, N1, and S3) for comparisons. Some solutions were also produced by weighting the rate pseudo-observations.

6. Results

6.1. Influence of the a Priori Model

We examine first the influence of the a priori nutation model on the estimation of nutation coefficients. Since only a limited number of nutation terms may be estimated, many terms are taken over from the a priori model without further improvement. The amplitude values adopted at these periods have an impact on amplitude estimates at nearby periods. Obviously, the IAU 1980 model is a bad candidate for an a priori model among other reasons because of the truncation of the coefficients to 0.1 mas and the neglect of terms with amplitudes below 0.05 mas. To assess the size of variations in the estimated amplitudes caused by a change of the a priori model, two identical solutions were performed, the only difference being the a priori models introduced, namely, the IERS96 model and the SKV972 model. The SKV972 model was determined using an analysis similar to that used for the IERS96 model but with the latest VLBI nutation offsets from Goddard Space Flight Center (GSFC) (Herring, private communication, 1997) (VBLI data from 1979 to mid 1997), and the latest *Souchay and Kinoshita* [1997] rigid-Earth nutation series. The differences in the estimated coefficients $\delta\psi_{rj}$, $\delta\psi_{ij}$, $\delta\epsilon_{rj}$, and $\delta\epsilon_{ij}$ between the two GPS solutions for all periods listed in Table 4 are shown in Figure 10 together with the corresponding GPS 1σ errors of the estimates (shaded area). The dashed line in Figure 10 represents the estimated precision of the amplitude estimates according to (33). The formal errors from the actual least squares adjustment are very well represented by a linear growth of the errors with the period. Deviations of the actual error bars from the dashed line indicate that neighboring periods are slightly correlated. The error bars of $\Delta\epsilon$ and $\Delta\psi \sin\epsilon_0$ are almost identical.

For all periods the differences in the estimated nutation coefficients are of the order of only a few microarcseconds (μas) and much smaller than the a posteriori errors of the coefficients resulting from the least squares adjustment. For all the results to follow we used the IERS96 model as a priori information.

Estimating semiannual and annual amplitudes in addition to the set of periods given in Table 4 in order to remove existing long-term variations led to changes of a few microarcseconds at the most in the nutation coefficients (at the "longer" periods between 10 and 16 days).

6.2. Influence of the Orbit Model and Rate Weighting

To study the impact of the orbit model on the nutation results, that part of the N3 series based uniquely on the new orbit model (day 273/1996 to day 300/1997) was analyzed separately and compared to the results using an equally long time period of the same series based on the old orbit model (244/1995 - 272/1996). For these much shorter series of only 394 days each, nutation coefficients were set up for a reduced set of 22 periods. These periods are flagged with an asterisk in Table 4.

The a posteriori RMS scatter of the nutation rate residuals for the two series is 0.25 mas/d and 0.28 mas/d, respectively. The difference between the two values is much smaller than the factor of 2–3 expected according to the formal errors of the rate estimates before and after the orbit model change (see Figure 6). This gives an indication that the formal errors of the rate values from the GPS data analysis are obviously not representative of the actual rate quality. This is confirmed by the circumstance, that annual and semiannual amplitude corrections (if also estimated as a diagnostic tool for orbit quality) are larger by a factor of 2–3 for the old orbit model than for the new one, much larger than the corresponding uncertainties. Using the formal errors to weight the rate values is therefore questionable and the RMS scatter derived from this orbit test might be a better measure. The two nutation components $\Delta\epsilon$ and $\Delta\psi \sin\epsilon_0$ contribute to the total RMS scatter with 0.20 and 0.26 mas/d, respectively, in the case of the old and with 0.29 and 0.24 mas/d in the case of the new orbit representation. Whereas the quality of the rates in obliquity suffer considerably from the new orbit model, the quality in longitude even seems to improve slightly.

Figure 11 shows the estimated nutation corrections relative to the IERS96 model for the two, short time series. They confirm that, although the formal errors are slightly larger for the new orbit model, the estimated coefficients are of the same quality for both orbit types, another reason to question the adequacy of the formal rate errors as a quality measure.

Both 394-day series already show a good agreement with the IERS96 theory of nutation (between 0 and 20 μas for short periods, below 100 μas for the longer periods). Only a few points are outside the 2σ confidence interval. When forming the differences between the two sets of coefficients,

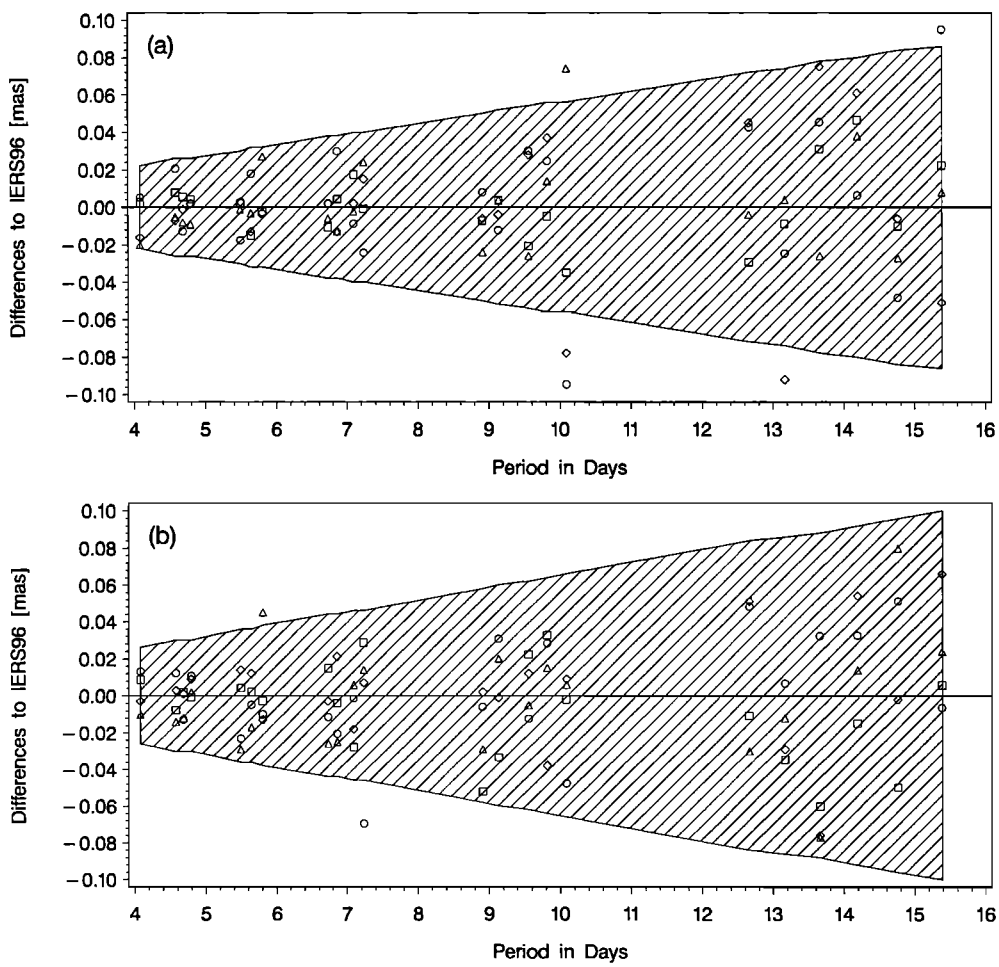

Figure 11. Nutation corrections relative to the IERS96 model for 22 periods estimated from a rate series of 394 days based on (a) the old orbit model and an equally long series based on (b) the new orbit model. Both series are parts of the N3 series. The shaded areas represent the 2σ error limits (95% confidence interval). Symbols as in Figure 10. Solid line, 2σ error band.

these differences are again within their 2σ confidence interval (which is $\sqrt{2}$ larger than for the individual sets). One discrepancy needs to be mentioned, however. If we compute the circular nutation components according to (40), we see that the term a_r^- for the 10.08-day period differs from the IERS96 value by 4 times its uncertainty. This only happens in the case of the old orbit model, whereas the corresponding result for the new orbit model does not show such an anomaly. Later we will see the same discrepancy in the analysis of the full N3 series, too.

The above results clearly show that, in general, nutation corrections of similar quality can be obtained with both orbit models. It is therefore not appropriate to use the rate uncertainties from the GPS analysis, which differ by a factor of 2–3 between the orbit models, to weight the rate estimates. Nevertheless, we computed a solution introducing the inverse of the squares of the formal errors as weights into the least squares procedure. As a result the amplitude differences compared to the IERS96 model increase. The deweighting of all results before January 1995 and after September 1996 has an effect comparable to a considerable shortening of the series. Stronger correlations between neighboring periods is also a consequence. The solutions to be presented next, making use of the full series N3, N1, and S3, were therefore generated without weighting the nutation rates.

6.3. Nutation Coefficients From the Series N3, N1, and S3

The set of 34 terms (136 coefficients) listed in Table 4 was determined from each of the three nutation rate series N3, N1, and S3. The corresponding RMS scatters of the postfit residuals are put together in Table 3. As expected from the formal errors of the rate estimates in Figure 6, the residuals are larger for solution types N1 and S3 than for N3, although the difference is not as pronounced as in Figure 6. We can infer that there is a considerable gain in quality when computing nutation rates from 3-day solutions instead of 1-day solutions. The higher noise level of series S3 is a consequence of the larger number of ERPs (2-hour resolution) and the higher correlations of these parameters with nutation rates. The noise level of the N3 rates with 0.27 mas/d is very similar to that of the UT1-UTC rates of about 20 μs/d estimated for these type of 3-day solutions. This shows that rates in UT1-UTC and in nutation can be determined with comparable quality.

Table 3. RMS of the Postfit Residuals of the Nutation Rates for the Three Series Defined in Table 1

Series	Number of Days	RMS in $\Delta\epsilon$, mas/d	RMS in $\Delta\psi \sin\epsilon_0$, mas/d
N3	1281	0.26	0.27
N1	1281	0.41	0.42
S3	1030	0.41	0.40

The estimated nutation corrections with respect to the values of the IERS96 nutation model are shown in Figure 12 for all three series together with the 95% confidence interval (2σ uncertainties). All figures have been drawn to the same scale for comparison. The a posteriori formal errors of the coefficients are smallest for the N3 series, and, although the RMS of the postfit residuals are almost identical for the N1 and S3 series, the formal errors of the coefficients from the S3 series are larger due to the shorter time interval it covers. We also see that the differences between the estimated coefficients and the IERS96 values are larger for the series N1 and even larger for S3 compared to the N3 series.

In view of the smaller formal errors of the N3 coefficients and the smaller differences with respect to the IERS96 values, we conclude that the rates from the N3 series give the best results (although we have to keep in mind the smoothing effect according to Figure 9). It should be pointed out, however, that within their respective error bars all three series give reasonable estimates for the coefficients compared to the IERS96 values. No systematic effects (e.g., from the subdaily ERP modeling or the lower time resolution of series N3 compared to N1) may be detected in the three series within the level of the 95% confidence interval.

The nutation corrections for the 34 periods resulting from the N3 series, the most promising series, are listed in Table 4, which also includes the values of the IERS96 and IAU 1980 models and the a posteriori formal errors of the coefficients. The a posteriori formal errors range from 7 and 17 μas at periods of about 4 days to 27 and 68 μas at 16 days for $\Delta\epsilon$ and $\Delta\psi$, respectively. The uncertainties of the circular nutation components (see (40)) vary from 5 to 19 μas over the same span of periods.

The major deficiencies of the IAU80 theory below periods of 20 days, already known from VLBI, can be seen by GPS. Especially, the significant change of the 13.66-day coefficients is very well recovered by GPS. We will have a closer look at the main periods (13.66 days, 9.13 days, ...) in the next section. This means that the GPS technique allows an independent verification of theoretical nutation models and of the results obtained by VLBI at the high-frequency range of the spectrum. Most of the nutation corrections from GPS relative to the IERS96 model lie within the 95% confidence interval which implies that the GPS nutation estimates are, in general, in good agreement with the IERS96 nutation model. The differences between GPS and IERS96 coefficients increase toward longer periods as anticipated in Figure 1 and indicated by the formal errors of the GPS estimates.

It is important to realize that the two components, $\Delta\epsilon$ and $\Delta\psi \sin\epsilon_0$, may be determined equally well from GPS. This is true from the point of view of the formal errors as well as from the amplitude differences with respect to the IERS96 model. If we remind ourselves of (16) we, indeed, do not expect any major difference between the two components concerning the impact of orbit modeling.

The standard deviations of the differences between the GPS and IERS96 coefficients over all 34 periods are 22, 16, 21, and 20 μas for the components $\psi_r \sin\epsilon_0$ (sin), $\psi_i \sin\epsilon_0$ (cos), ϵ_r (cos), and ϵ_i (sin), respectively, or 20 μas over all

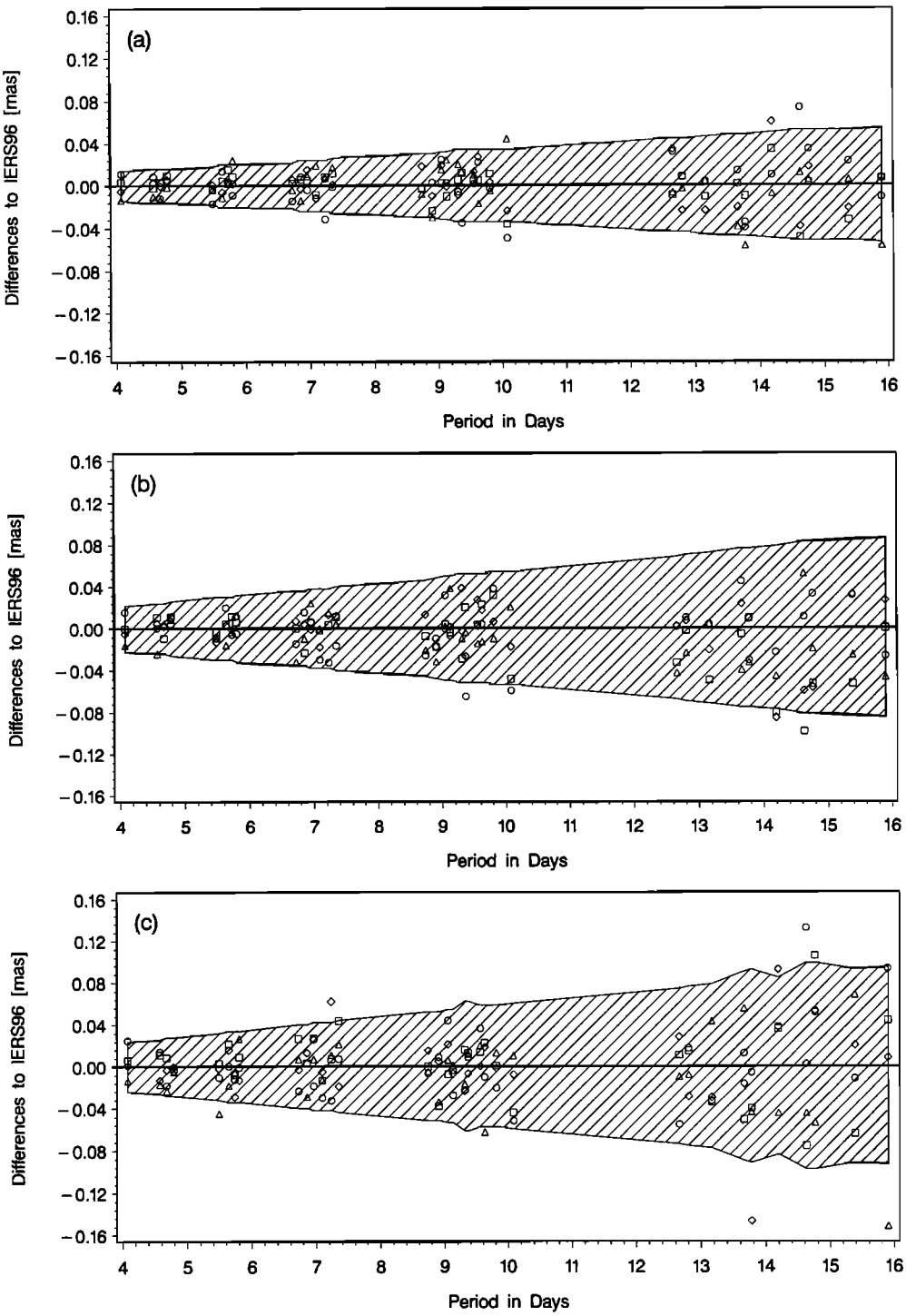

Figure 12. Nutation corrections relative to the IERS96 model for 34 periods estimated from the rate series N3, N1, and S3 characterized in Table 1. The shaded areas represent the 95% confidence interval. Solid line, 2σ error band. Symbols as in Figure 10. (a) Nutation corrections from rate series N3, (b) nutation corrections from rate series N1, and (c) nutation corrections from rate series S3.

components. Because the differences (together with the formal errors) are growing linearly with the period (see Figure 12a), a more appropriate measure of the agreement between the two sets of coefficients is given by the median of the absolute values of the differences. The median values for the four components amount to 12, 8, 12, and 10 μas, showing an mean agreement over all 136 coefficients of about 10 μas.

The largest deviations from the IERS96 model show up in $\Delta\psi$ at the 10.08-day and 14.63-day periods with differences of about 3 times their formal uncertainties. From a statistical point of view we may expect a few coefficients of the total of 136 to lie outside the 95% confidence interval. The deviation at 10.08 days is most probably an artifact because it only appears in the results from the old but not the new orbit model (see Figure 11).

Table 4. Nutation Corrections in $\Delta\epsilon$ and $\Delta\psi$ Relative to the IERS96 Model for 34 Periods

Multiple of					Period,	Reduced	Component	I96,	I80,	I80-I96,	GPS-I96,	σ,
l	l'	F	D	Ω	days	Set		μas	μas	μas	μas	μas
1	0	2	4	2	4.08	*	ψ_r	-16	0	16	29	17
							ψ_i	0	0	0	10	17
							ϵ_r	7	0	-7	-13	7
							ϵ_i	0	0	0	-5	7
4	0	2	0	2	4.58	*	ψ_r	-26	0	26	22	19
							ψ_i	0	0	0	-5	20
							ϵ_r	11	0	-11	-10	8
							ϵ_i	0	0	0	3	8
2	0	2	2	2	4.68	*	ψ_r	-108	-100	8	-29	20
							ψ_i	1	0	-1	9	20
							ϵ_r	47	0	-47	-13	8
							ϵ_i	0	0	0	0	8
0	0	2	4	2	4.79	*	ψ_r	-69	-100	-31	11	20
							ψ_i	0	0	0	25	20
							ϵ_r	29	0	-29	-1	8
							ϵ_i	0	0	0	6	8
3	0	2	0	2	5.49	*	ψ_r	-289	-300	-11	-42	23
							ψ_i	2	0	-2	-9	23
							ϵ_r	124	100	-24	-3	9
							ϵ_i	1	0	-1	1	9
1	0	2	2	2	5.64	*	ψ_r	-768	-800	-32	35	24
							ψ_i	4	0	-4	11	24
							ϵ_r	325	300	-25	-11	10
							ϵ_i	2	0	-2	-6	10
1	-1	2	2	2	5.73		ψ_r	-59	0	59	10	25
							ψ_i	0	0	0	38	25
							ϵ_r	25	0	-25	2	10
							ϵ_i	0	0	0	3	10
-1	0	2	4	2	5.80	*	ψ_r	-151	-200	-49	-22	25
							ψ_i	1	0	-1	22	25
							ϵ_r	66	100	34	24	10
							ϵ_i	0	0	0	2	10
2	1	2	0	2	6.73	*	ψ_r	40	0	-40	-36	29
							ψ_i	0	0	0	6	29
							ϵ_r	-17	0	17	-4	11
							ϵ_i	0	0	0	6	11
2	0	2	0	2	6.86	*	ψ_r	-3102	-3100	2	21	30
							ψ_i	12	0	-12	15	30
							ϵ_r	1323	1300	-23	-14	12
							ϵ_i	5	0	-5	-3	12
0	1	2	2	2	6.96		ψ_r	54	0	-54	-10	30
							ψ_i	0	0	0	12	30
							ϵ_r	-22	0	22	9	12
							ϵ_i	0	0	0	15	12
0	0	2	2	2	7.10	*	ψ_r	-3854	-3800	54	-29	31
							ψ_i	15	0	-15	-21	31
							ϵ_r	1643	1600	-43	19	12
							ϵ_i	6	0	-6	-12	12
0	-1	2	2	2	7.24	*	ψ_r	-264	-300	-36	-79	31
							ψ_i	1	0	-1	21	31
							ϵ_r	114	100	-14	7	12
							ϵ_i	0	0	0	7	12
-2	0	2	4	2	7.35		ψ_r	-121	-100	21	-3	31
							ψ_i	0	0	0	29	31
							ϵ_r	52	100	48	17	13
							ϵ_i	0	0	0	1	13
3	0	2	-2	2	8.75		ψ_r	94	100	6	-7	37
							ψ_i	0	0	0	-8	37
							ϵ_r	-40	0	40	-8	15
							ϵ_i	0	0	0	18	15
1	1	2	0	2	8.91	*	ψ_r	246	200	-46	7	39
							ψ_i	-1	0	1	-60	39
							ϵ_r	-106	-100	6	-30	15
							ϵ_i	0	0	0	-10	15

Table 4. (continued)

Multiple of					Period,	Reduced	Component	I96,	I80,	I80-I96,	GPS-I96,	σ,
l	l'	F	D	Ω	days	Set		μas	μas	μas	μas	μas
-1	0	4	0	2	9.06		ψ_r	115	100	-15	61	39
							ψ_i	0	0	0	5	39
							ϵ_r	-49	0	49	15	16
							ϵ_i	0	0	0	19	16
1	0	2	0	2	9.13	*	ψ_r	-30137	-30100	37	6	40
							ψ_i	77	0	-77	-26	40
							ϵ_r	12896	12900	4	24	16
							ϵ_i	35	0	-35	-1	16
-1	1	2	2	2	9.31		ψ_r	56	0	-56	-15	42
							ψ_i	0	0	0	13	42
							ϵ_r	-24	0	24	20	17
							ϵ_i	0	0	0	-9	17
1	-1	2	0	2	9.37		ψ_r	-287	-300	-13	-88	42
							ψ_i	1	0	-1	30	42
							ϵ_r	123	100	-23	13	17
							ϵ_i	0	0	0	-1	17
-1	0	2	2	2	9.56	*	ψ_r	-5965	-5900	65	4	42
							ψ_i	14	0	-14	13	42
							ϵ_r	2554	2600	46	10	17
							ϵ_i	7	0	-7	13	17
1	0	0	2	1	9.63		ψ_r	-95	-100	-5	55	42
							ψ_i	0	0	0	12	42
							ϵ_r	49	0	-49	-17	17
							ϵ_i	0	0	0	27	17
-1	-1	2	2	2	9.81	*	ψ_r	-282	-300	-18	-8	43
							ψ_i	1	0	-1	28	43
							ϵ_r	122	100	-22	-5	17
							ϵ_i	0	0	0	3	17
-1	0	0	4	0	10.08	*	ψ_r	133	100	-33	-124	43
							ψ_i	0	0	0	-91	43
							ϵ_r	-4	0	4	44	17
							ϵ_i	0	0	0	-24	17
0	0	4	-2	2	12.66	*	ψ_r	91	100	9	79	55
							ψ_i	0	0	0	-23	55
							ϵ_r	-39	0	39	-7	22
							ϵ_i	0	0	0	34	22
2	0	2	-2	2	12.81		ψ_r	643	600	-43	19	55
							ψ_i	-1	0	1	20	55
							ϵ_r	-277	-300	-23	-3	22
							ϵ_i	0	0	0	-24	22
0	1	2	0	2	13.17	*	ψ_r	757	700	-57	9	57
							ψ_i	-1	0	1	-27	57
							ϵ_r	-326	-300	26	4	23
							ϵ_i	0	0	0	-24	23
0	0	2	0	2	13.66	*	ψ_r	-227720	-227400	320	34	61
							ψ_i	269	0	-269	3	61
							ϵ_r	97864	97700	-164	-39	24
							ϵ_i	136	0	-136	-21	24
2	0	0	0	0	13.78		ψ_r	2923	2900	-23	-88	61
							ψ_i	-8	0	8	-26	62
							ϵ_r	-62	-100	-38	-57	24
							ϵ_i	1	0	-1	-40	24
0	-1	2	0	2	14.19	*	ψ_r	-714	-700	14	24	62
							ψ_i	1	0	-1	85	62
							ϵ_r	307	300	-7	-8	25
							ϵ_i	0	0	0	60	25
-2	0	2	2	2	14.63		ψ_r	139	100	-39	184	65
							ψ_i	0	0	0	-124	65
							ϵ_r	-60	-100	-40	12	26
							ϵ_i	0	0	0	-39	26
0	0	0	2	0	14.77	*	ψ_r	6336	6300	-36	85	66
							ψ_i	-15	0	15	6	66
							ϵ_r	-125	-200	-75	5	26
							ϵ_i	3	0	-3	17	26

Table 4. (continued)

Multiple of					Period,	Reduced	Component	I96,	I80,	I80-I96,	GPS-I96,	σ,
l	l'	F	D	Ω	days	Set		μas	μas	μas	μas	μas
0	-1	0	2	0	15.39	*	ψ_r	435	400	-35	56	66
							ψ_i	-1	0	1	-83	66
							ϵ_r	-9	0	9	5	26
							ϵ_i	0	0	0	-22	26
-2	0	0	4	0	15.91		ψ_r	128	100	-28	-29	68
							ψ_i	0	0	0	16	68
							ϵ_r	1	0	-1	-57	27
							ϵ_i	0	0	0	7	27

The GPS values were determined from the rate series N3 relative to the IERS96 model. The values of the IERS96 (I96) model, the IAU80 theory of nutation (I80), and the difference between the two are also listed. The asterisks in column "Reduced Set" indicate the periods considered when using the reduced set of terms (see text). The a posteriori formal uncertainties σ of the estimated nutation corrections are given in the last column.

The residual spectrum of the nutation rate observations after the estimation of the 34 terms is shown in Figure 13. It has been scaled the same way as Figure 8 for easy comparison. It shows that there remain a few spectral lines with amplitudes on the level of about twice the formal uncertainties. One lines appears at a period of about 10.37 days (a^+) and could be associated with the term $Nj = (-1, -1, 0, 4, 0)$. We already mentioned above the relatively large discrepancy between the GPS estimate and the IERS96 model in the case of the 10.08-day period. The deviations around 10 days might be caused by the old orbit model, although the actual mechanism is unclear. Other lines are located at 9.73 days (a^+) and 7.5 days (a^-), for neither of which we expect any large amplitude according to theory. It is certainly too early to speculate about their origin. First, the whole series of nutation rate solutions should be recomputed with a consistent and optimized orbit model. We close this section with the remark that these remaining lines are more noticeable in the $\Delta\psi$ than in the $\Delta\epsilon$ component.

6.4. Comparison of Individual Periods With Different Models

We have seen that the overall agreement between the IERS96 model values and the GPS-derived amplitudes is at a level of approximately 10 μas (median). Let us now compare GPS results of the major nutation periods in more detail with results from VLBI and LLR published recently. Because nutation analyses using VLBI and LLR data are mostly focussing on longer periods than those considered here, we may only compare the amplitude estimates for a few periods, namely, 13.66, 9.13, 14.77, and 9.56 days with more than one source.

Before going into a detailed comparison let us look at three factors, using the 13.66-day term as an example, that may have an impact on the amplitude estimates: (1) the change in the coefficients of the 13.66-day period depending on whether or not we estimate the neighboring term at 13.78 days (the closer 13.63-day period cannot be separated from the 13.66-day period), (2) how much the amplitudes are

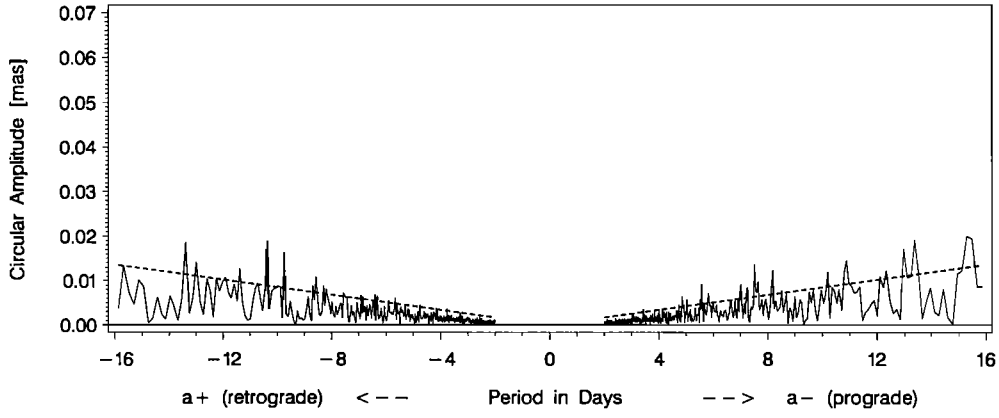

Figure 13. Residual spectrum of circular nutation amplitudes at low periods generated from the series N3 relative to the IERS96 model after the estimation of nutation coefficients for 34 periods (see Table 4). The dashed lines indicate the 1σ uncertainties of the amplitude estimations.

Table 5. Impact of Various Error Sources on the 13.66-Day Nutation Corrections Estimated From GPS

Error Source	Changes in Coefficients, μas			
	$\delta\psi_r$ (sin)	$\delta\psi_i$ (cos)	$\delta\epsilon_r$ (cos)	$\delta\epsilon_i$ (sin)
With, without estimating 13.78 term	-24	4	-9	-16
With, without smoothing	-16	13	8	7
A priori SKV972 or IERS96	7	-3	-8	-1
Formal uncertainties from GPS	61	61	24	24

reduced by the smoothing effect discussed in section 5.2, and (3) the change produced by a change of the a priori model from IERS96 to SKV972.

Table 5 summarizes the result of these potential "error sources." The amplitude changes due to factors (1) and (3) were obtained by computing corresponding solutions. Figure 9 tells us that the amplitudes at 13.66 days are reduced by 5% for 3-day rates. This leads to the numbers given in Table 5, that is, about 5% of the differences between the IERS96 and the IAU80 model, assuming that the IERS96 coefficients are more or less correct. All three effects are small compared with the formal uncertainties of the GPS estimates shown in the bottom row of Table 5. The largest change is caused by estimating or not estimating the neighboring term at 13.78 days. When comparing the results of individual spectral lines below, we should therefore keep in mind that the amplitudes estimated at a specific frequency critically depend on the amplitudes adopted for all the neighboring lines of the nutation spectrum.

Apart from the IAU 1980 theory of nutation (IAU80) [*McCarthy*, 1996], the IERS 1996 model (IERS96) [*McCarthy*, 1996], and the latest model by Souchay and Kinoshita (SKV972: see section 6.1 for details), the nutation coefficients from *McCarthy and Luzum* [1991] (MCLU91: combined analysis of 10 years of VLBI and about 20 years of LLR data), *Herring et al.* [1991] (HERR91: 9 years of VLBI data), *Charlot et al.* [1995] (CHAR95: 16 years of VLBI and 24 years of LLR data), *Souchay et al.* [1995] (SOUC95: 14 years of VLBI data) and the GPS results of series N3 (GPS_N3) are put together in Table 6 for those

Table 6. Comparison of the Nutation Coefficients Derived From GPS With Theoretical Models and Estimates From VLBI and LLR

Nutation Model	Period, days	Nutation Coefficient, mas							
		$\delta\psi_r$ (sin)		$\delta\psi_i$ (cos)		$\delta\epsilon_r$ (cos)		$\delta\epsilon_i$ (sin)	
IAU80	13.66	-227.4		0.0		97.7		0.0	
MCLU91		-227.94	±0.12	-0.07	±0.11	98.00	±0.06	-0.10	±0.04
HERR91		-228.19	±0.14	0.10	±0.14	98.03	±0.06	-0.08	±0.06
CHAR95		-227.35	±0.12	-0.07	±0.11	97.66	±0.05	0.04	±0.05
SOUC95		-227.71	±0.04	0.34	±0.04	97.85	±0.01	0.17	±0.01
IERS96		-227.720		0.269		97.864		0.136	
SKV972		-227.643		0.289		97.836		0.146	
GPS_N3		-227.686	±0.061	0.272	±0.061	97.825	±0.024	0.115	±0.024
IAU80	9.13	-30.1		0.0		12.9		0.0	
MCLU91		-30.33	±0.05	-0.09	±0.09	12.96	±0.02	-0.01	±0.03
HERR91		-30.34	±0.14	0.03	±0.14	12.97	±0.06	0.07	±0.06
CHAR95		-30.03	±0.08	0.03	±0.09	13.00	±0.03	0.07	±0.03
SOUC95		-30.20	±0.04	0.06	±0.04	12.91	±0.01	0.11	±0.01
IERS96		-30.137		0.077		12.896		0.035	
SKV972		-30.127		0.081		12.892		0.037	
GPS_N3		-30.131	±0.040	0.051	±0.040	12.920	±0.016	0.034	±0.016
IAU80	14.77	6.3		0.0		-0.2		0.0	
HERR91		6.41	±0.14	-0.10	±0.14	-0.19	±0.06	0.00	±0.06
SOUC95		6.35	±0.03	-0.08	±0.03	-0.13	±0.01	0.00	±0.01
IERS96		6.336		-0.015		-0.125		0.003	
SKV972		6.335		-0.016		-0.123		0.003	
GPS_N3		6.421	±0.066	-0.009	±0.066	-0.120	±0.026	0.020	±0.026
IAU80	9.56	-5.9		0.0		2.6		0.0	
SOUC95		-5.99	±0.03	0.06	±0.03	2.57	±0.01	0.00	±0.01
IERS96		-5.965		0.014		2.554		0.007	
SKV972		-5.961		0.015		2.552		0.007	
GPS_N3		-5.961	±0.042	0.027	±0.042	2.564	±0.017	0.020	±0.017

Table 7. Comparison of the Circular Nutation Coefficients Derived From GPS With Theoretical Models and Estimates From VLBI and LLR

Nutation Model	Period, days	Nutation Coefficient, mas							
		a_r^+ (cos)		a_i^+ (sin)		a_r^- (cos)		a_i^- (sin)	
IERS96	13.66	-3.641		-0.014		-94.223		0.122	
SKV972		-3.642		-0.016		-94.194		0.130	
GPS_N3		-3.628	±0.017	-0.003	±0.017	-94.197	±0.017	0.112	±0.017
IERS96	9.13	-0.454		-0.002		-12.442		0.033	
SKV972		-0.454		-0.002		-12.438		0.035	
GPS_N3		-0.467	±0.011	-0.007	±0.011	-12.453	±0.011	0.027	±0.011
IERS96	14.77	-1.198		-0.004		1.323		-0.001	
SKV972		-1.198		-0.005		1.321		-0.002	
GPS_N3		-1.217	±0.019	-0.012	±0.019	1.337	±0.019	0.008	±0.019
IERS96	9.56	-0.091		-0.001		-2.463		0.006	
SKV972		-0.090		-0.001		-2.462		0.006	
GPS_N3		-0.096	±0.012	-0.005	±0.012	-2.467	±0.012	0.015	±0.012

periods below 20 days that are available in the respective publications. For completeness and easier comparisons with publications expressing nutation corrections in the circular components (see equations (40)), we also list the circular terms for the models IERS96, SKV972, and GPS_N3 in Table 7.

The uncertainties of the GPS estimates in Table 6 are smaller than most of the VLBI uncertainties. An exception is SOUC95, the uncertainties of which are better by a factor 1–2 (depending on the period). Only two of the 34 GPS_N3 terms show a deviation of more than the formal uncertainty from both, IERS96 and SKV972, namely $\delta\epsilon_r$ at 9.13 days and $\delta\psi_r$ at 14.77 days. To get an impression of the agreement of the models in Table 6 with SKV972, probably the best model presently available, we computed the standard deviation of the differences between two models for all nutation components (the $\Delta\psi$ components were multiplied by $\sin\epsilon_0$) and determined the maximum difference between the two models. These values are listed in Table 8 for all models with respect to SKV972. Let us keep in mind that the results of such a comparison are not fully independent of the a priori nutation model used for each of the individual solutions. We see that the agreement of the GPS estimates with SKV972 for the four periods considered here is very good compared to the other models. We thus conclude that GPS (1) gives an independent confirmation of the quality of the SKV972 model and (2) can contribute significantly to nutation at high frequencies. It also seems that GPS nutation results are less sensitive to the modeling of other diurnal rotation changes (e.g., the diurnal UT1 variations) than VLBI most likely because of the more global distribution of stations with GPS (see *Herring and Dong* [1994] for discussion of VLBI sensitivity). A change of the diurnal UT1 variation model led, for example, to the difference in the a_r^- term of the 13.66-day period between IERS96 and SKV972 (see Table 7).

Table 8. Agreement Between SKV972 and All Other Models Listed in Table 6 Measured by the Maximum Difference Between SKV972 and the Respective Model and by the Standard Deviation of the Differences Over All Periods and All Terms ($\delta\epsilon_r$, $\delta\epsilon_i$, $\delta\psi_r \sin\epsilon_0$, and $\delta\psi_i \sin\epsilon_0$)

Nutation Model	Number of Terms	Standard Deviation, mas	Maximum, mas
IAU80	16	0.068	0.146
MCLU91	8	0.132	0.246
HERR91	12	0.117	0.226
CHAR95	8	0.107	0.176
SOUC95	16	0.025	0.073
IERS96	16	0.011	0.030
GPS_N3	16	0.016	0.034

7. Conclusions

It is well known that a direct determination of UT1-UTC corrections from satellite geodetic data is not possible. For several years, however, satellite techniques (SLR, GPS, Doppler orbitography and radiopositioning integrated by satellite (DORIS), ...) have been used to estimate UT1-UTC rates (or LOD). We have shown that from a mathematical point of view there is no major difference between estimating UT1-UTC rates and nutation rates in obliquity $\Delta\epsilon$ and longitude $\Delta\psi$ from satellite geodetic measurements. For all three components of Earth rotation it is not possible to determine offsets to an a priori model because of the one-to-one correlations with the geometrical orbit parameters (ascending node, inclination, and argument of latitude), whereas the first derivative of these quantities with respect to time can be estimated.

The nutation rate series analyzed in this paper are the first nutation series established in satellite geodesy. The series were computed from GPS data of the global IGS network by the CODE analysis center of the IGS using 3-day solutions. The series of daily nutation rate estimates was started in spring 1994 and it covers to date more than 3.5 years. The RMS scatter of the nutation rate estimates is about 0.27 mas/d (in $\Delta\epsilon$ and $\Delta\psi \sin\epsilon_0$) and is thus comparable

to the 20 μs/d scatter of the LOD values derived from GPS 3-day solutions.

It is evident that such rate estimates may only contribute at the high-frequency end of the nutation spectrum, the long-term behavior being reserved to VLBI (and to LLR) analyses. We demonstrated, however, that corrections to an a priori nutation model may successfully be estimated for terms with periods up to about 16 days from GPS nutation rates. The uncertainties of the nutation coefficients are of about the same magnitude for $\Delta\epsilon$ and $\Delta\psi \sin\epsilon_0$ and grow linearly with the associated period from typically several microarcseconds at periods of a few days to about 30 μas at periods of about 16 days.

The coefficients of 34 nutation periods between 4 and 16 days were derived from the GPS rate series and show an overall agreement of about 10 μas (median) or 20 μas (standard deviation) with the latest nutation models available from Souchay and Kinoshita. The comparison of the GPS coefficients for the larger nutation terms at 13.66, 9.13, 14.77, and 9.56 days with values found in the literature shows that the GPS results represent a significant contribution to nutation in this range of frequencies. No major discrepancies were found between the most recent model by Souchay and Kinoshita (1997.2) and the GPS estimates for these frequencies. The deficiencies in the IAU 1980 model are clearly seen. GPS thus allows an independent verification of present-day nutation models. The high-frequency nutations depend almost solely on the elastic and anelastic properties of the mantle through the parameter R' in (33) of the theory by *Mathew et al.* [1991]. This coefficient is most affected by the k_2 Love number. The expected contributions from anelasticity are given by *Herring et al.* [1991] and are still debated. They could be of the order of 1%, that is, for the 13.66-day nutation with an amplitude of about 100 mas we might expect effects of about 1% of 100 mas times R' or about 20 μas (with $R' \approx 0.25/13.66$ [*Mathew et al.*, 1991]). GPS nutation results may be of value in this area of research and in the search for potential ocean normal modes [*Herring and Dong*, 1994].

It is our hope that in the future other GPS groups or other satellite space techniques will follow this example and start to estimate nutation rates in their analyses. It would then be possible to derive nutation corrections from a combination of different series stemming from VLBI, LLR, GPS, and other satellite systems.

Acknowledgment. We thank the GSFC VLBI group for making available to us the nutation offset series from VLBI.

References

Aoki, S., and H. Kinoshita, Note on the relation between the equinox and Guinot's non-rotating origin, *Celestial Mech.*, *29*, 335–360, 1983.

Bartel, N., T. A. Herring, M. I. Ratner, I. I. Shapiro, and B. E. Corey, VLBI limits on the proper motion of the "core" of the superluminal quasar 3C 345, *Nature*, *319*, 733–737, 1986.

Beutler, G., Himmelsmechanik II: Der erdnahe Raum, Mitteilungen der Satelliten-Beobachtungsstation Zimmerwald, *Rep. 28*, Astron. Inst., Univ. of Berne, Berne, Switzerland, 1991.

Beutler, G., I. I. Mueller, and R. E. Neilan, The International GPS Service for Geodynamics (IGS): Development and start of official service on January 1, 1994, *Bull. Géod.*, *68*(1), 39–70, 1994a.

Beutler, G., E. Brockmann, W. Gurtner, U. Hugentobler, L. Mervart, and M. Rothacher, Extended orbit modeling techniques at the CODE Processing Center of the International GPS Service for Geodynamics (IGS): Theory and initial results, *Manuscr. Geod.*, *19*, 367–386, 1994b.

Beutler, G., R. Weber, U. Hugentobler, M. Rothacher, and A. Verdun, GPS satellite orbits, in *Lecture Notes International School "GPS for Geodesy"*, Springer-Verlag, New York, 1996a.

Beutler, G., E. Brockmann, U. Hugentobler, L. Mervart, M. Rothacher, and R. Weber, Combining consecutive short arcs into long arcs for precise and efficient GPS orbit determination, *J. Geod.*, *70*, 287–299, 1996b.

Botton, S., M. Rothacher, T. Springer, and G. Beutler, Reprocessing of about 15 months of global IGS data using an improved orbit model, *Rep. CM 38*, Lab. de Rech. Géod., Institut Géographique National, Paris, 1997.

Boucher, C., Z. Altamimi, M. Feissel, and P. Sillard, Results and analysis of the ITRF94, *IERS Technical Note 20*, Cent. Bur. of Int. Earth Rotation Serv., Obs. de Paris, 1996.

Brockmann, E., Combination of solutions for geodetic and geodynamic applications of the Global Positioning System (GPS), Ph.D. thesis, Geod.-geophys Arb. in der Schweiz, *55*, Zurich, Switzerland, 1997.

Charlot, P., O. J. Sovers, J. G. Williams, and X. X. Newhall, Precession and nutation from joint analysis of radio interferometric and lunar laser ranging observations, *Astron. J.*, *109*(1), 418–427, 1995.

Feissel, M., and L. Castrique (Eds.), 1996 IERS annual report, pp. II–73, Cent. Bur. of Int. Earth Rotation Serv., Obs. de Paris, 1997.

Fliegel, H. F., T. E. Gallini, and E. R. Swift, Global Positioning System radiation force model for geodetic applications, *Geophys. Res. Lett.*, *97*(B1), 559–568, 1992.

Gambis, D., Multi-technique EOP combination, in *Proceedings of the 1996 IGS Analysis Center Workshop, Silver Spring, Maryland*, edited by R. E. Neilan et al., pp. 61–70, IGS Cent. Bur., Jet Propul. Lab., Pasadena, Calif., 1995.

Herring, T. A., and D. Dong, Measurement of diurnal and semidiurnal rotational variations and tidal parameters of Earth, *J. Geophys. Res.*, *99*(B9), 18051–18071, 1994.

Herring, T. A., B. A. Buffett, P. M. Mathews, and I. I. Shapiro, Forced nutations of the Earth: Influence of inner core dynamics, 3, Very long interferometry data analysis, *J. Geophys. Res.*, *96*(B5), 8259–8273, 1991.

Kinoshita, H., Theory of the Rotation of the Rigid Earth, *Celestial Mech.*, *15*, 277–326, 1977.

Kouba, J., and Y. Mireault, 1997 Analysis Coordinator Report, in *IGS 1997 Annual Report*, edited by J. F. Zumberge and R. E. Neilan, IGS Cent. Bur., Jet Propul. Lab., Pasadena, Calif., in press, 1998.

Mathew, P. M., B. A. Buffett, T. A. Herring, and I. I. Shapiro, Forced nutations of the Earth: Influence of inner core dynamics, 3, Theory, *J. Geophys. Res.*, *96*(B5), 8219–8242, 1991.

McCarthy, D. D., IERS Conventions (1996), *IERS Tech. Note 21*, Obs. de Paris, 1996.

McCarthy, D. D., and B. J. Luzum, Observations of luni-solar and free core nutation, *Astron. J.*, *102*(5), 1889–1895, 1991.

Mervart, L., Ambiguity resolution techniques in geodetic and geodynamic applications of the Global Positioning System, Ph.D. thesis, Geod.-geophys. Arb. in der Schweiz, *53*, Zurich, Switzerland, 1995.

Ray, R. D., D. J. Steinberg, B. F. Chao, and D. E. Cartwright, Diurnal and semidiurnal variations in the Earth's rotation rate induced by oceanic tides, *Science*, *264*, 830–832, 1994.

Rothacher, M., and L. Mervart, *The Bernese GPS Software Version 4.0*, Astron. Inst., Univ. of Berne, Berne, Switzerland, 1996.

Rothacher, M., G. Beutler, and L. Mervart, The perturbation of the orbital elements of GPS satellites through direct radiation pressure, in *IGS Workshop Proceedings on Special Topics and New Directions*, edited by G. Gendt and G. Dick, pp. 152–166, GeoForschungsZentrum, Potsdam, Germany, 1995.

Rothacher, M., T. A. Springer, S. Schaer, G. Beutler, E. Brockmann, U. Wild, A. Wiget, C. Boucher, S. Botton, and H. Seeger, Annual report 1996 of the CODE Processing Center of the IGS, in *IGS 1996 Annual Report*, edited by J. F. Zumberge et al., pp. 201–219, IGS Cent. Bur., Jet Propul. Lab., Pasadena, Calif., 1997.

Saastamoinen, J., Atmospheric correction for the troposphere and stratosphere in radio ranging of satellites, in *The Use of Artificial Satellites for Geodesy, Geophys. Monogr. Ser.*, vol. 15, edited by S. W. Henriksen et al., pp. 247–251, AGU, Washington, D. C., 1971.

Seidelmann, P. K., 1980 IAU nutation: The final report of the IAU Working Group on Nutation, *Celestial Mechanics*, *27*, 79–106, 1982.

Souchay, J., and H. Kinoshita, Corrections and new developments in rigid-earth nutation theory, II, Influence of second-order geopotential and direct planetary effect, *Astron. Astrophys.*, *318*, 639–652, 1997.

Souchay, J., M. Feissel, C. Bizouard, N. Capitaine, and M. Bougeard, Precession and nutation for a non-rigid Earth: Comparison between theory and VLBI observations, *Astron. Astrophys.*, *299*, 277–287, 1995.

Sovers, O. J., C. S. Jacobs, and R. S. Gross, Measuring rapid ocean tidal earth orientation variations with very long baseline interferometry, *J. Geophys. Res.*, *98*(B11), 19959–19971, 1993.

Springer, T. A., M. Rothacher, and G. Beutler, Using the extended CODE orbit model: First experiences, in *IGS 1996 Analysis Center Workshop*, edited by R. E. Neilan et al., pp. 13–25, Cent. Bur., Jet Propul. Lab., Pasadena, Calif., 1996.

Springer, T. A., G. Beutler, and M. Rothacher, Improving the orbit estimates of the GPS satellites, *J. Geod.*, 1998, in press.

Tapley, B. D., B. E. Schutz, R. J. Eanes, J. C. Ries, and M. M. Watkins, Lageos laser ranging contributions to geodynamics, geodesy, and orbital dynamics, in *Contributions of Space Geodesy to Geodynamics: Earth Dynamics, Geodyn. Ser.*, vol. 24, edited by D. E. Smith and D. L. Turcott, pp. 147–173, AGU, Washington, D. C., 1993.

Wahr, J. M., The forced nutation of an elliptical, rotating, elastic, and oceanless earth, *Geophys. J. R. Astron. Soc.*, *64*, 705–727, 1981.

Watkins, M. M., and R. Eanes, Diurnal and semidiurnal variations in Earth orientation determined from LAGEOS laser ranging, *J. Geophys. Res.*, *99*(B9), 18073–18079, 1994.

Weber, R., Monitoring earth orientation variations at the Center for Orbit Determination in Europe (CODE), *Österreichische Z. Vermessung und Geoinformation*, *84*(3), 269–275, 1996.

Zumberge, J. F., D. E. Fulton, and R. E. Neilan (Eds.), *1996 Annual Report of the International GPS Service for Geodynamics*, IGS Cent. Bur., Jet Propul. Lab., Pasadena, Calif., 1997.

G. Beutler and M. Rothacher, Astronomical Institute, University of Berne, Sidlerstrasse 5, CH-3012 Berne, Switzerland. (gerhard.beutler@aiub.unibe.ch; markus.rothacher@aiub.unibe.ch)

T. A. Herring, Department of Earth, Atmospheric and Planetary Sciences, Massachusetts Institute of Technology, 77 Massachusetts Avenue, Rm 54-620, Cambridge, MA 02139. (tah@mtglas.mit.edu)

R. Weber, Department of Theoretical Geodesy, University of Technology Vienna, Gusshausstrasse 27-29, Vienna A-1040, Austria. (rweber@terra.tuwien.ac.at)

(Received March 11, 1998; revised September 30, 1998; accepted October 19, 1998.)